

## Supplementary Information

### **Hf-based Metal-Organic Frameworks as acid-base catalysts for the transformation of biomass-derived furanic compounds into chemicals**

Sergio Rojas-Buzo, Pilar García-García,\* Avelino Corma\*

Instituto de Tecnología Química, UPV-CSIC, Universitat Politècnica de València-Consejo Superior de Investigaciones Científicas. Avenida de los Naranjos s/n 46022 Valencia, Spain.

Email: pgargar@itq.upv.es; acorma@itq.upv.es

#### **Experimental section. General Information.**

Unless otherwise stated, all reagents were purchased from commercial suppliers and used without further purification. Solvents employed in the reactions were purified using a solvent purification system (SPS) MBraun 800. Organic solutions were concentrated under reduced pressure on a Büchi rotary evaporator. Reactions were monitored by thin layer chromatography on silica gel pre-coated aluminium plates using fluorescence quenching with UV light at 254 nm or KMnO<sub>4</sub>. Flash column chromatography was performed using E. Merck silica gel (60, particle size 0.040-0.063 mm). Chemical yields refer to pure isolated substances unless stated otherwise. All the products obtained were characterised by GC-MS, <sup>1</sup>H- and <sup>13</sup>C-NMR, and DEPT. When available, characterisation given in the literature was used for comparison. Gas chromatographic analyses were performed in an instrument equipped with a 25 m capillary column of 5% phenylmethylsilicone using dodecane as an external standard otherwise indicated. GC/MS analyses were performed on a spectrometer equipped with the same column as the GC and operated under the same conditions. <sup>1</sup>H and <sup>13</sup>C NMR were recorded on a Bruker 300 spectrometer and the chemical shifts are reported in ppm relative to residual proton solvents signals. Data for <sup>1</sup>H NMR spectra are reported as follows: chemical shift ( $\delta$ , ppm), multiplicity (s = singlet, d = doublet, t = triplet, q = quartet, m = multiplet, dd = double doublets), coupling constant and integration. Data for <sup>13</sup>C NMR spectra are reported in chemical shift ( $\delta$ , ppm). C, N, and H contents were determined with a Carlo Erba 1106 elemental analyzer. Thermogravimetric and differential thermal analysis (TGA-DTA) were conducted in an air stream with a Metler Toledo TGA/SDTA 851E analyzer. Solid state MAS-NMR spectra were recorded at room temperature under magic angle spinning (MAS) in a Bruker AV-400 spectrometer. The <sup>13</sup>C cross-polarization (CP) spectrum was acquired by using a 7 mm Bruker BL-7 probe and at a sample spinning rate of 5kHz. <sup>13</sup>C was referred to adamantane. FTIR spectra were recorded with a Nicolet 710 spectrometer (4 cm<sup>-1</sup> resolution) using conventional greaseless cell. IR spectra of the organic precursors were recorded on KBr disks at room temperature or by impregnating the windows with a dichloromethane solution of the compound and leaving to evaporate before analysis.

## 1. Synthesis of Zr- and Hf-based MOFs and characterization

1.1. **UiO-66(Hf)**: It was prepared according to the reported method in the literature.<sup>[1]</sup>

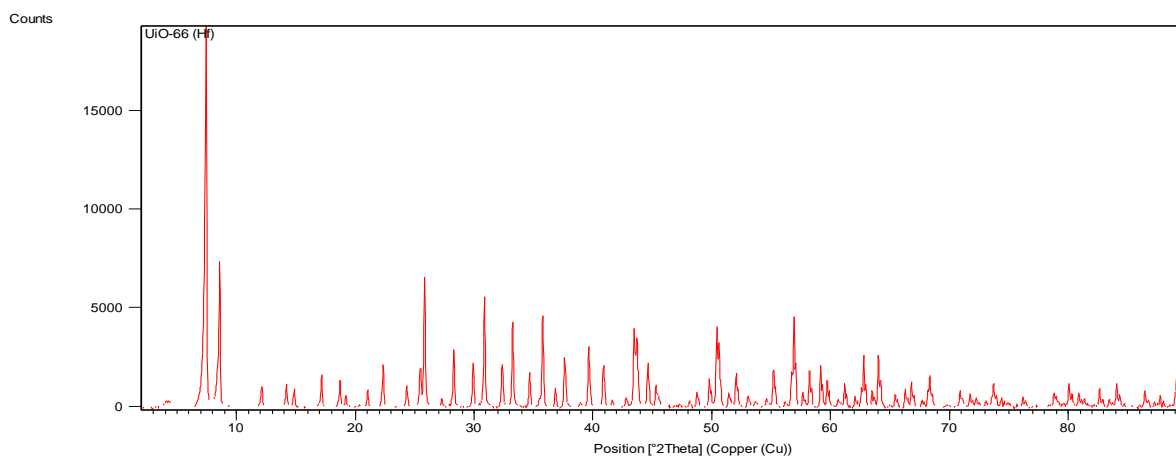
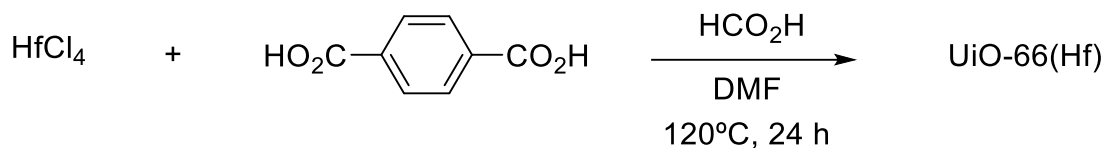


Figure S1. XRD pattern of UiO-66 (Hf)

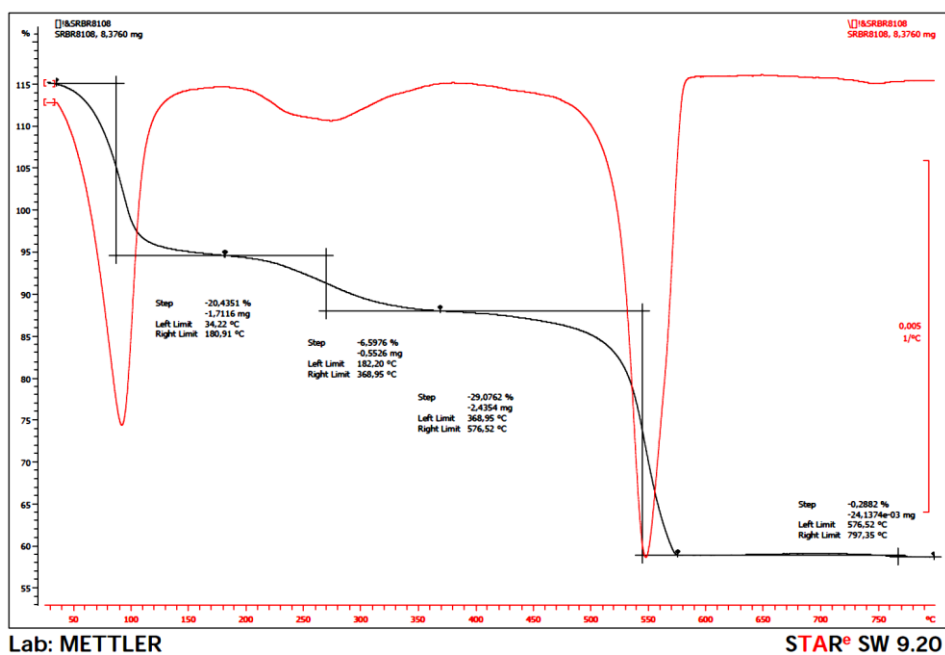
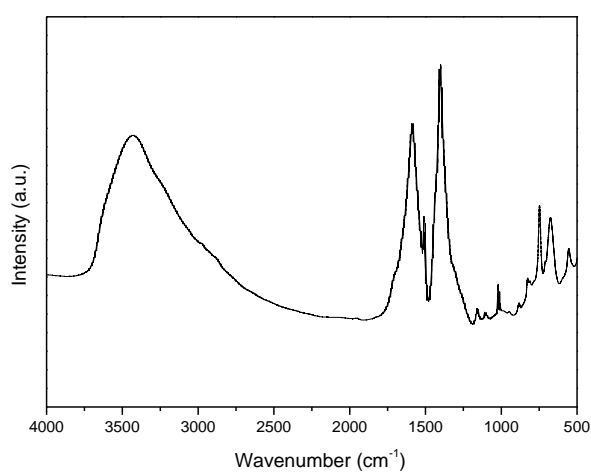


Figure S2. TGA and DTA curves of UiO-66 (Hf) sample.

**Table S1.** Chemical analysis of UiO-66 (Hf) sample.

Sample	Org.Cont. <sup>a</sup>					
	C <sup>a</sup>	H <sup>a</sup>	N <sup>a</sup>	Metal <sup>b</sup>	CHN <sup>c</sup>	TGA <sup>d</sup>
UiO-66 (Hf)	20.2	1.6	0.2	44	22	35.7

<sup>a</sup> Percentage in weight (%wt); <sup>b</sup>Determined by ICP analysis <sup>c</sup>Organic content from CHNS elemental analysis, <sup>d</sup>Organic content from thermogravimetical analysis without taking into account hydration water.



**Figure S3.** FTIR spectrum of UiO-66 (Hf) sample

**Table S2.** Textural Characteristic of UiO-66 (Hf).

Sample	BET Surface Area/m <sup>2</sup> g <sup>-1</sup>	Total Pore Volume/cm <sup>3</sup> g <sup>-1</sup>
UiO-66 (Hf).	584	0.45

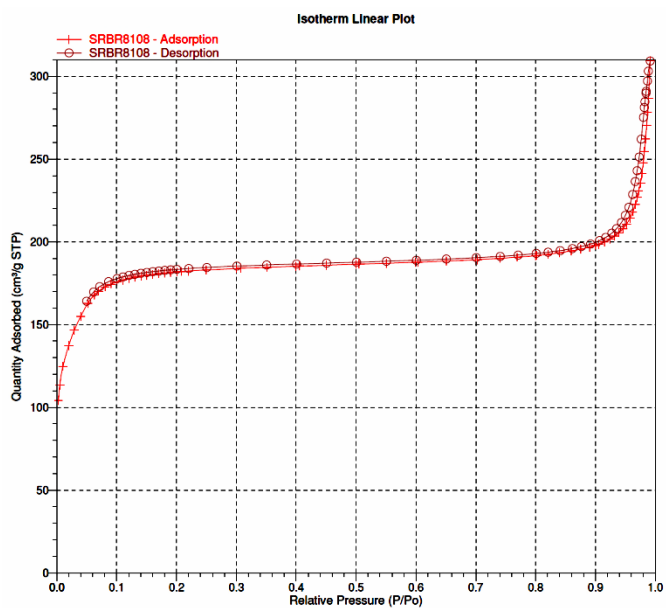


**Figure S4.** N<sub>2</sub> adsorption and desorption isotherm of UiO-66 (Hf) sample

**1.2. UiO-66 (Zr):** UiO-66-Zr was obtained by the same procedure<sup>[1]</sup> as for UiO-66 (Hf) except ZrCl<sub>4</sub> was used instead of HfCl<sub>4</sub>.

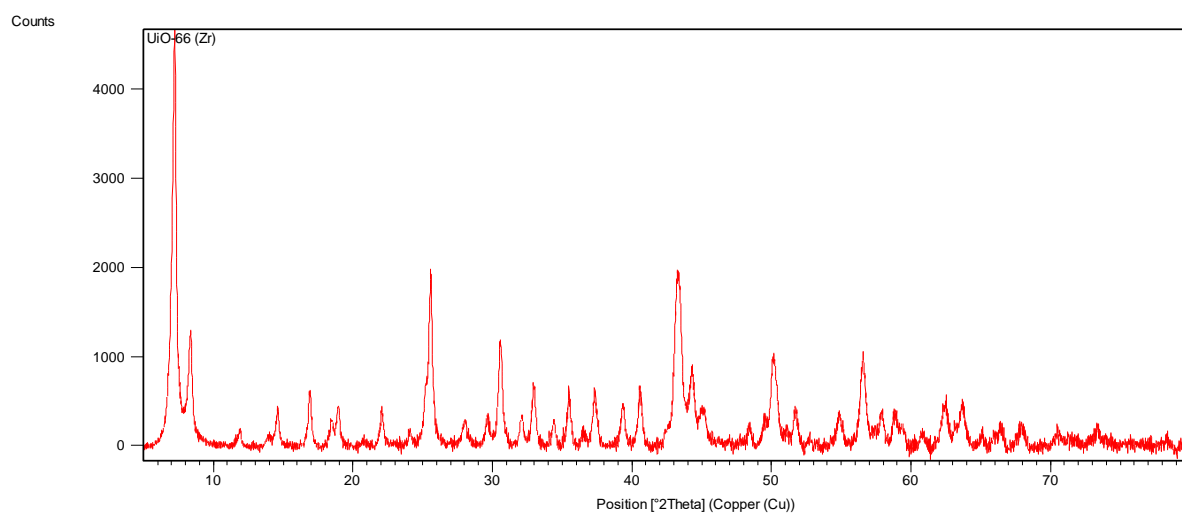
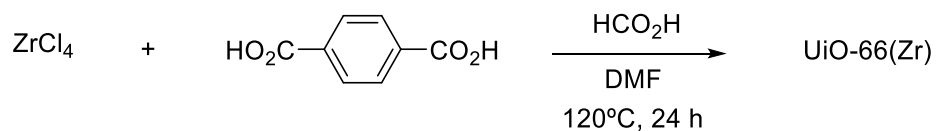


**Figure S5.** XRD pattern of UiO-66 (Zr)

**Table S3.** Chemical analysis of UiO-66 (Zr) sample.

Sample	Org.Cont. <sup>a</sup>					
	C <sup>a</sup>	H <sup>a</sup>	N <sup>a</sup>	Metal <sup>b</sup>	CHN <sup>c</sup>	TGA <sup>d</sup>
UiO-66 (Zr)	26.8	1.9	0.5	28	29.2	47.5

<sup>a</sup> Percentage in weight (%wt); <sup>b</sup>Determined by ICP analysis <sup>c</sup>Organic content from CHNS elemental analysis, <sup>d</sup>Organic content from thermogravimetric analysis without taking into account hydration water.

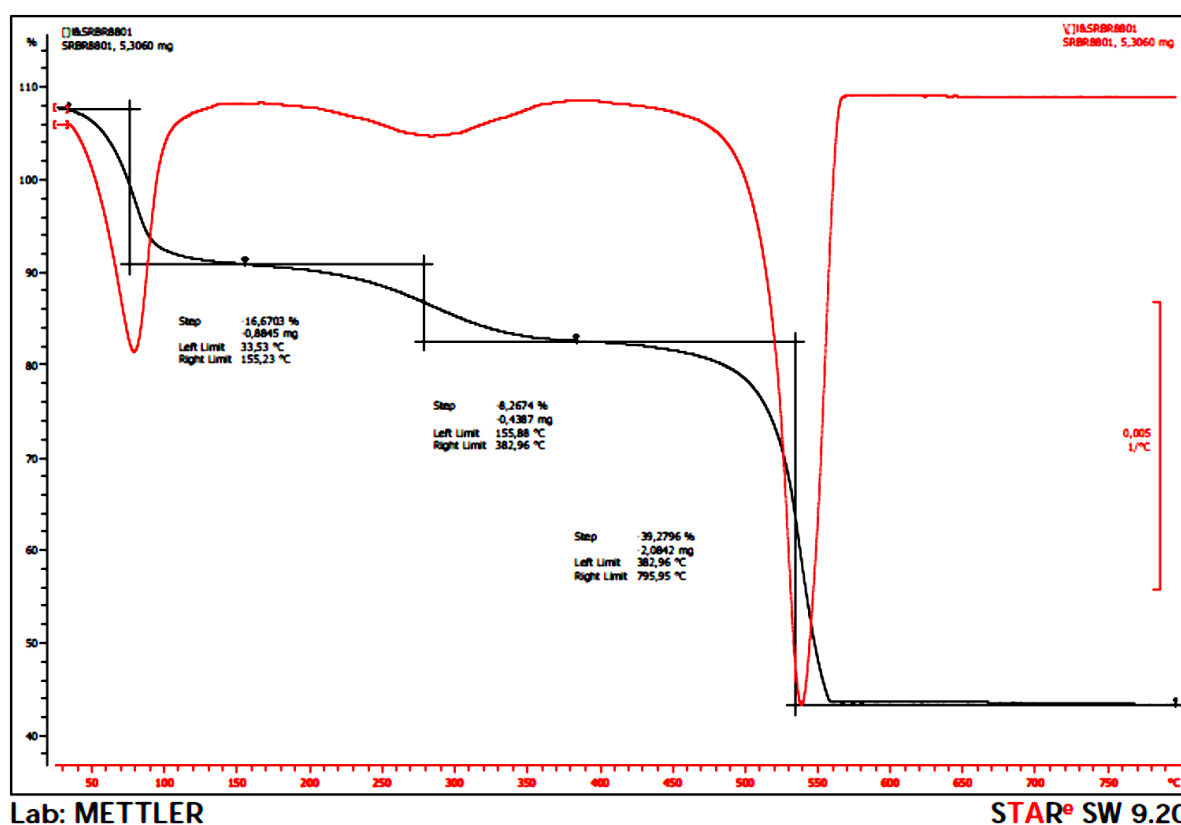


**Figure S6.** TGA and DTA curves of UiO-66 (Zr) sample.

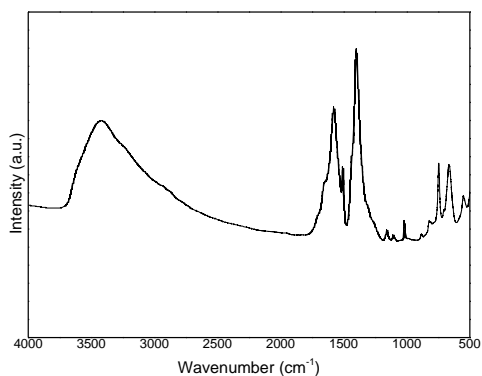


**Figure S7.** FTIR spectrum of UiO-66 (Zr) sample

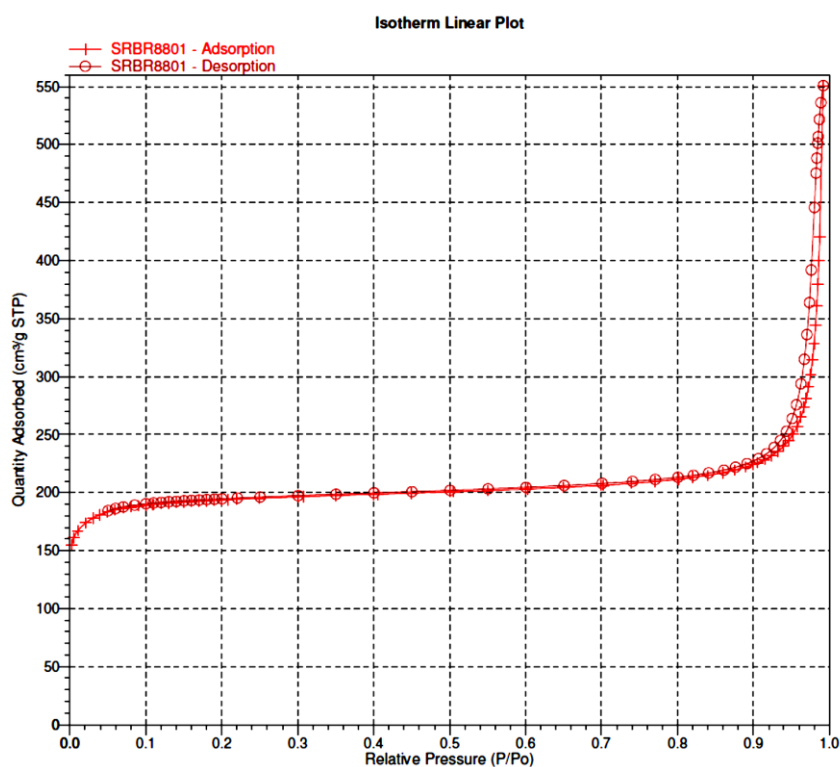


**Figure S8.** N<sub>2</sub> adsorption and desorption isotherm of UiO-66 (Zr) sample

**Table S4.** Textural Characteristic of UiO-66 (Zr).

Sample	BET Surface Area/m <sup>2</sup> g <sup>-1</sup>	Total Pore Volume/cm <sup>3</sup> g <sup>-1</sup>
UiO-66 (Zr).	619	0.78

**1.3. UiO-66-NH<sub>2</sub>(Hf):** UiO-66-NH<sub>2</sub>(Hf) was obtained by the same procedure<sup>[1]</sup> as for UiO-66 (Hf) except 2-aminoterephthalic acid was used instead of terephthalic acid.

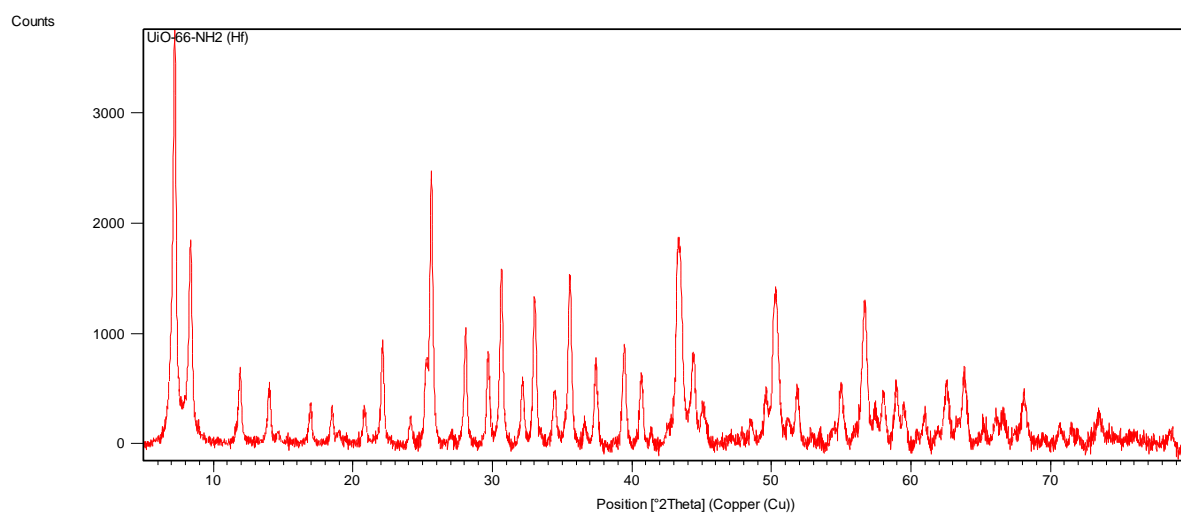
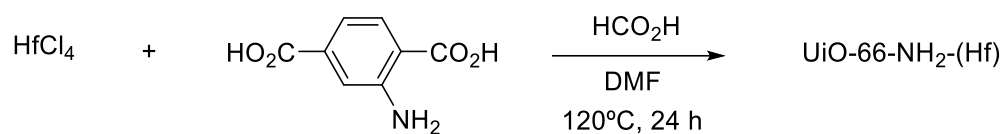


**Figure S9.** XRD pattern of UiO-66-NH<sub>2</sub> (Hf)

**Table S5.** Chemical analysis of UiO-66-NH<sub>2</sub> (Hf) sample.

Sample	C <sup>a</sup>	H <sup>a</sup>	N <sup>a</sup>	Metal <sup>b</sup>	Org.Cont. <sup>a</sup>	
					CHN <sup>c</sup>	TGA <sup>d</sup>
UiO-66-NH <sub>2</sub> (Hf)	20.1	2.1	2.8	38	25	40

<sup>a</sup> Percentage in weight (%wt); <sup>b</sup>Determined by ICP analysis <sup>c</sup>Organic content from CHNS elemental analysis, <sup>d</sup>Organic content from thermogravimetric analysis without taking into account hydration water.

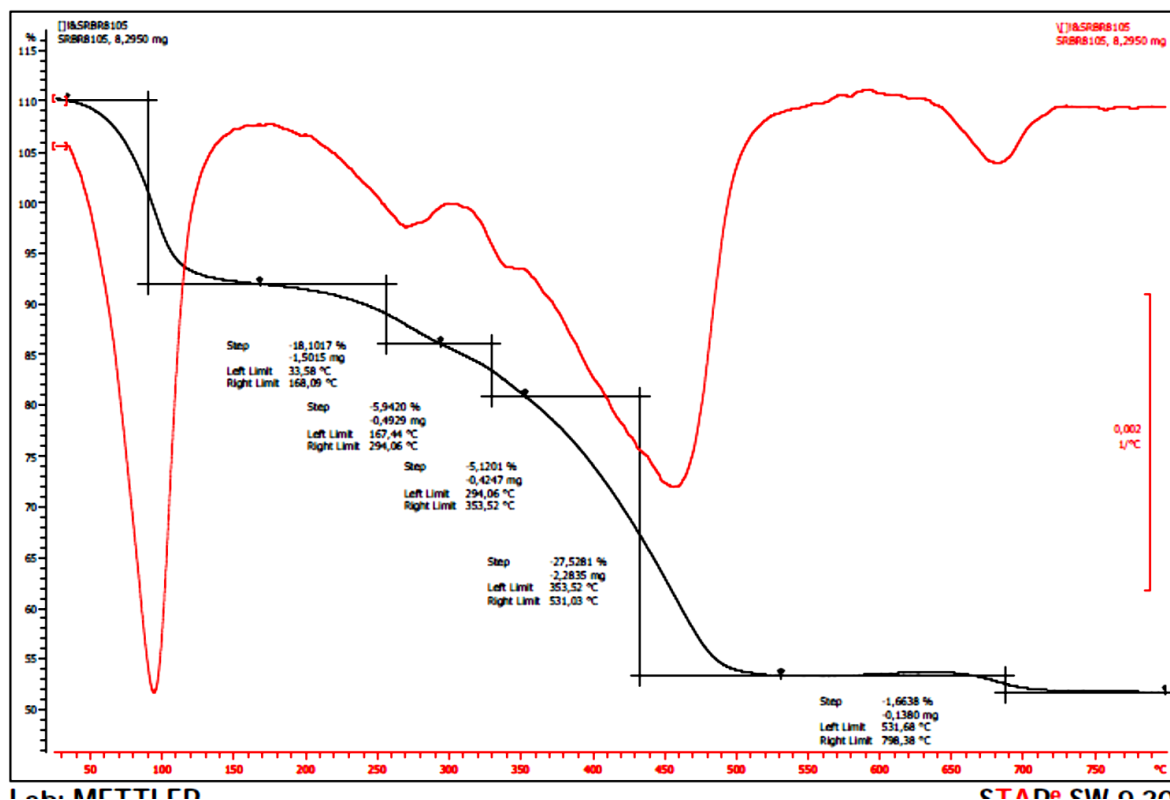


Figure S10. TGA and DTA curves of UiO-66-NH<sub>2</sub> (Hf) sample.

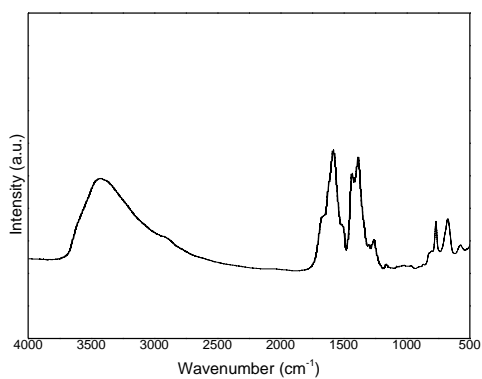
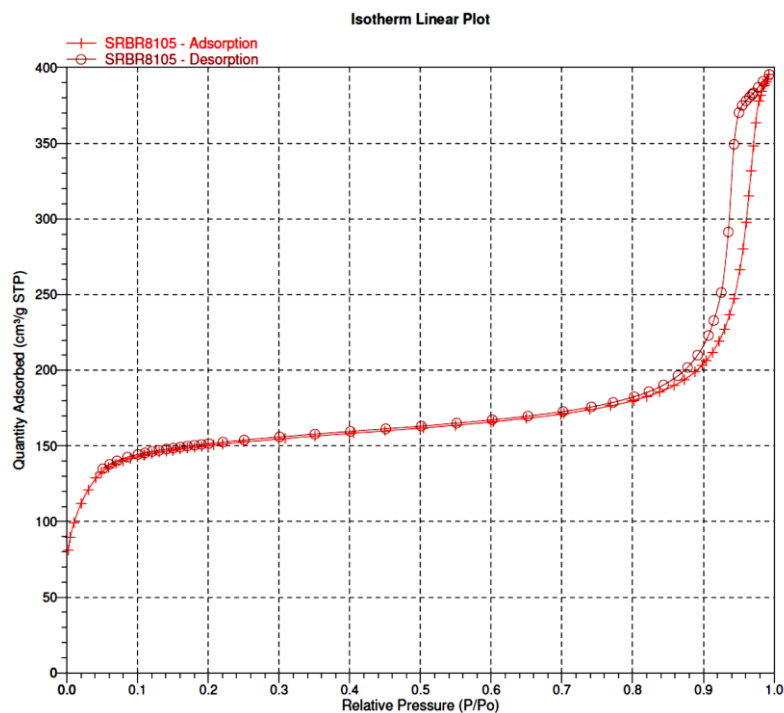


Figure S11. FTIR spectrum of UiO-66-NH<sub>2</sub> (Hf) sample



**Figure S12.** N<sub>2</sub> adsorption and desorption isotherm of UiO-66-NH<sub>2</sub> (Hf) sample

**Table S6.** Textural Characteristic of UiO-66-NH<sub>2</sub> (Hf)

Sample	BET Surface Area/m <sup>2</sup> g <sup>-1</sup>	Total Pore Volume/cm <sup>3</sup> g <sup>-1</sup>
UiO-66-NH <sub>2</sub> (Hf)	490	0.60

**1.4. UiO-67 (Hf)** It was prepared according to the reported method in the literature [2]

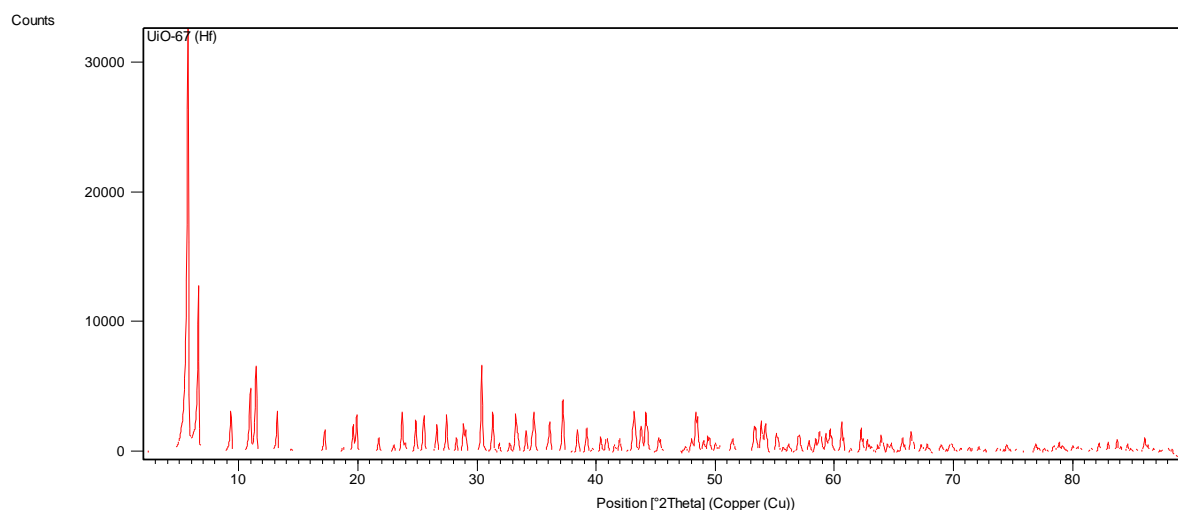
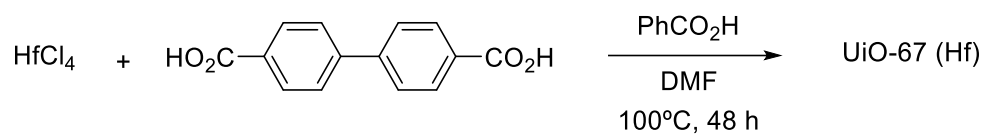


**Figure S13.** XRD pattern of UiO-67 (Hf)

**Table S7.** Chemical analysis of UiO-67 (Hf) sample.

Sample	C <sup>a</sup>	H <sup>a</sup>	N <sup>a</sup>	Metal <sup>b</sup>	Org.Cont. <sup>a</sup>	
					CHN <sup>c</sup>	TGA <sup>d</sup>
UiO-67 (Hf)	35.7	2.4	0.2	37	38.3	47

<sup>a</sup> Percentage in weight (%wt); <sup>b</sup>Determined by ICP analysis <sup>c</sup>Organic content from CHNS elemental analysis, <sup>d</sup>Organic content from thermogravimetric analysis without taking into account hydration water.

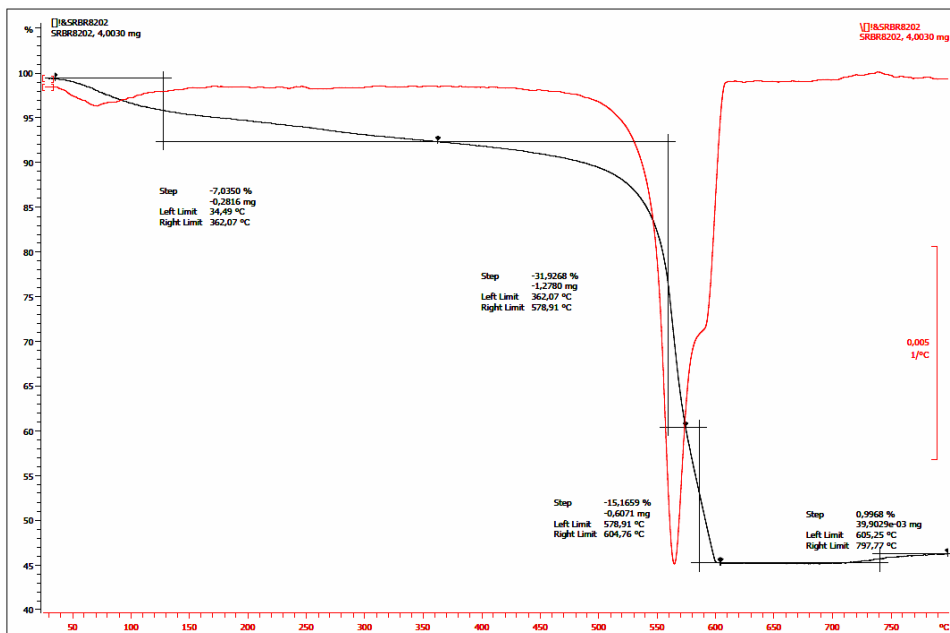


Figure S14. TGA and DTA curves of UiO-67 (Hf) sample.

1.5. Hf-MOF-808: It was prepared according to the reported method in the literature [2]

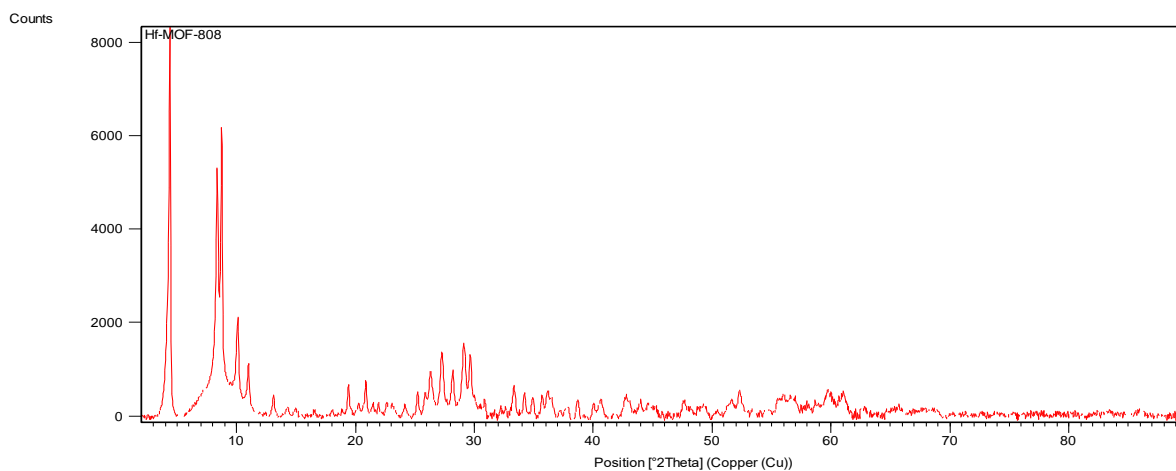
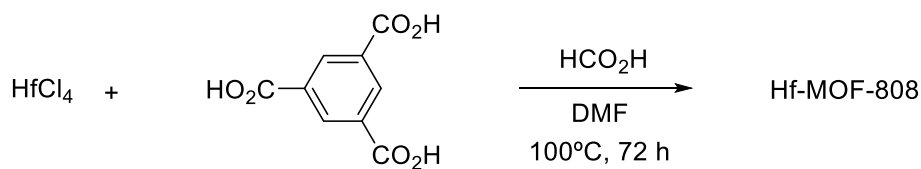
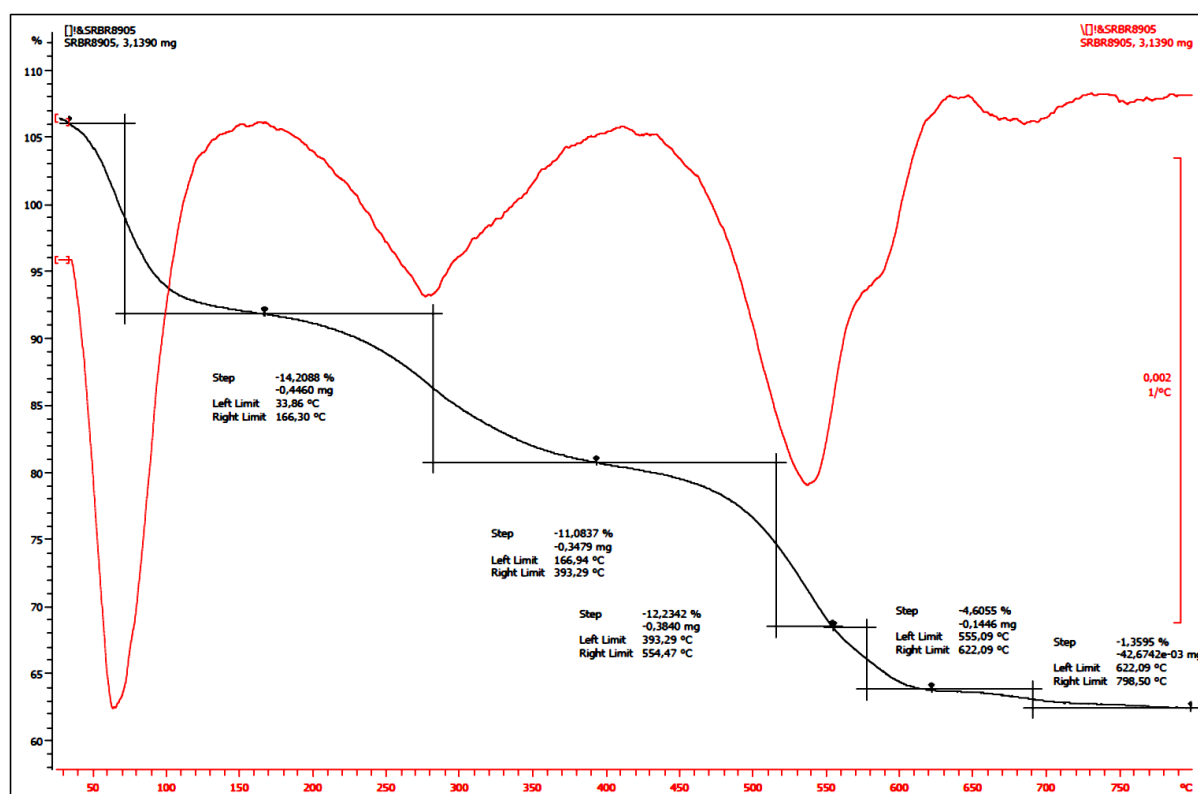


Figure S15. XRD pattern of Hf-MOF-808

**Table S8.** Chemical analysis of Hf-MOF-808 sample.

Sample	Org.Cont. <sup>a</sup>					
	C <sup>a</sup>	H <sup>a</sup>	N <sup>a</sup>	Metal <sup>b</sup>	CHN <sup>c</sup>	TGA <sup>d</sup>
Hf-MOF-808	13.9	1.3	0.3	46	15.5	29

<sup>a</sup> Percentage in weight (%wt); <sup>b</sup>Determined by ICP analysis <sup>c</sup>Organic content from CHNS elemental analysis, <sup>d</sup>Organic content from thermogravimetric analysis without taking into account hydration water.



**Figure S16.** TGA and DTA curves of Hf-MOF-808 sample.

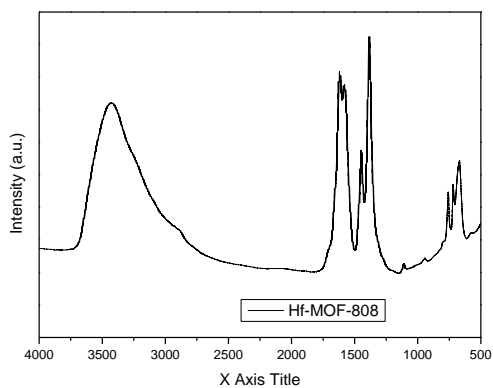


**Figure S17.** FTIR spectrum of Hf-MOF-808 sample

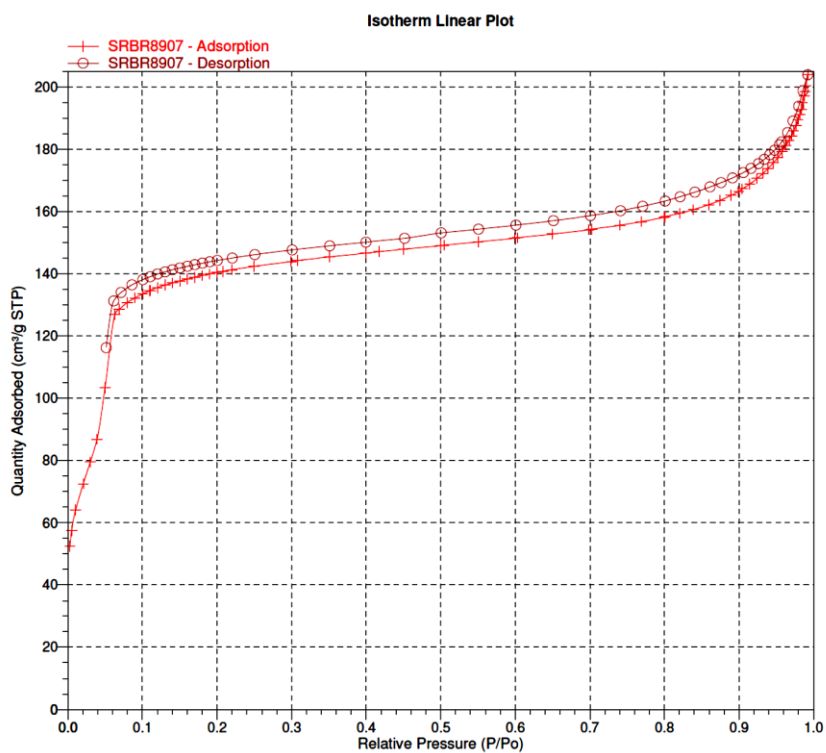


**Figure S18.** N<sub>2</sub> adsorption and desorption isotherm of Hf-MOF-808 sample

**Table S9.** Textural Characteristic of Hf-MOF-808.

Sample	BET Surface Area/m <sup>2</sup> g <sup>-1</sup>	Total Pore Volume/cm <sup>3</sup> g <sup>-1</sup>
Hf-MOF-808	458	0.30

**1.6. Zr-MOF-808:** Zr-MOF-808 was obtained by the same procedure<sup>[2]</sup> as for Hf-MOF-808 except ZrCl<sub>4</sub> was used instead of HfCl<sub>4</sub>.

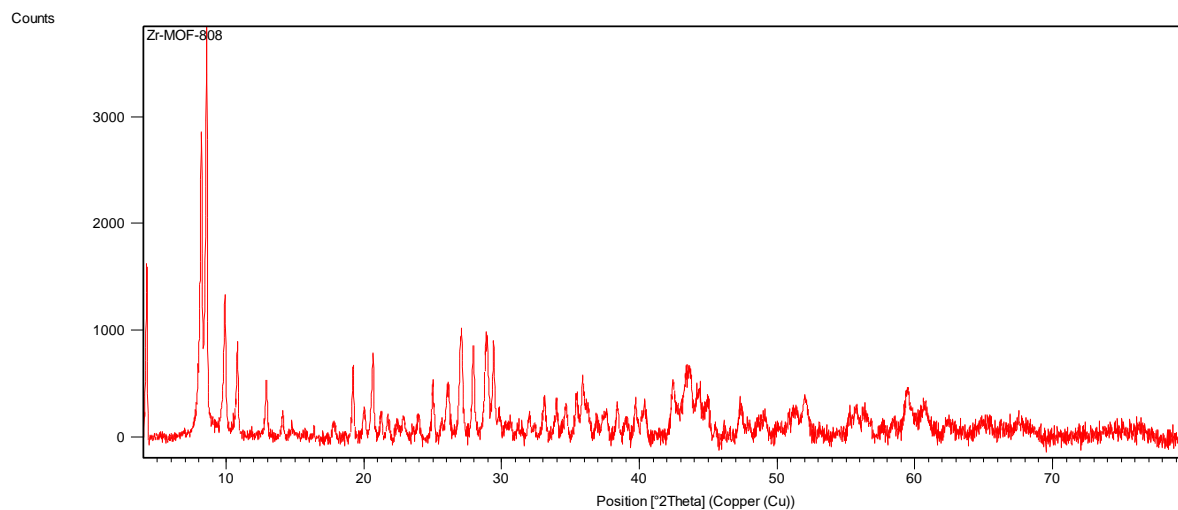
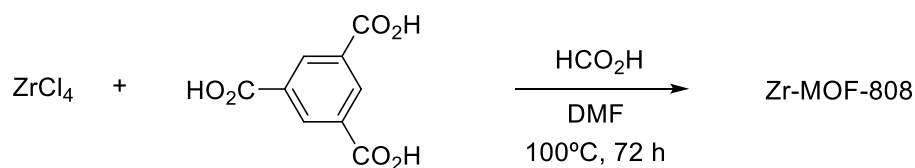


**Figure S19.** XRD pattern of Zr-MOF-808

**Table S10.** Chemical analysis of Zr-MOF-808 sample.

Sample	C <sup>a</sup>	H <sup>a</sup>	N <sup>a</sup>	Metal <sup>b</sup>	Org.Cont. <sup>a</sup>	
					CHN <sup>c</sup>	TGA <sup>d</sup>
Zr-MOF-808	19.6	2.7	1.1	31	23.4	42

<sup>a</sup> Percentage in weight (%wt); <sup>b</sup>Determined by ICP analysis <sup>c</sup>Organic content from CHNS elemental analysis, <sup>d</sup>Organic content from thermogravimetric analysis without taking into account hydration water.

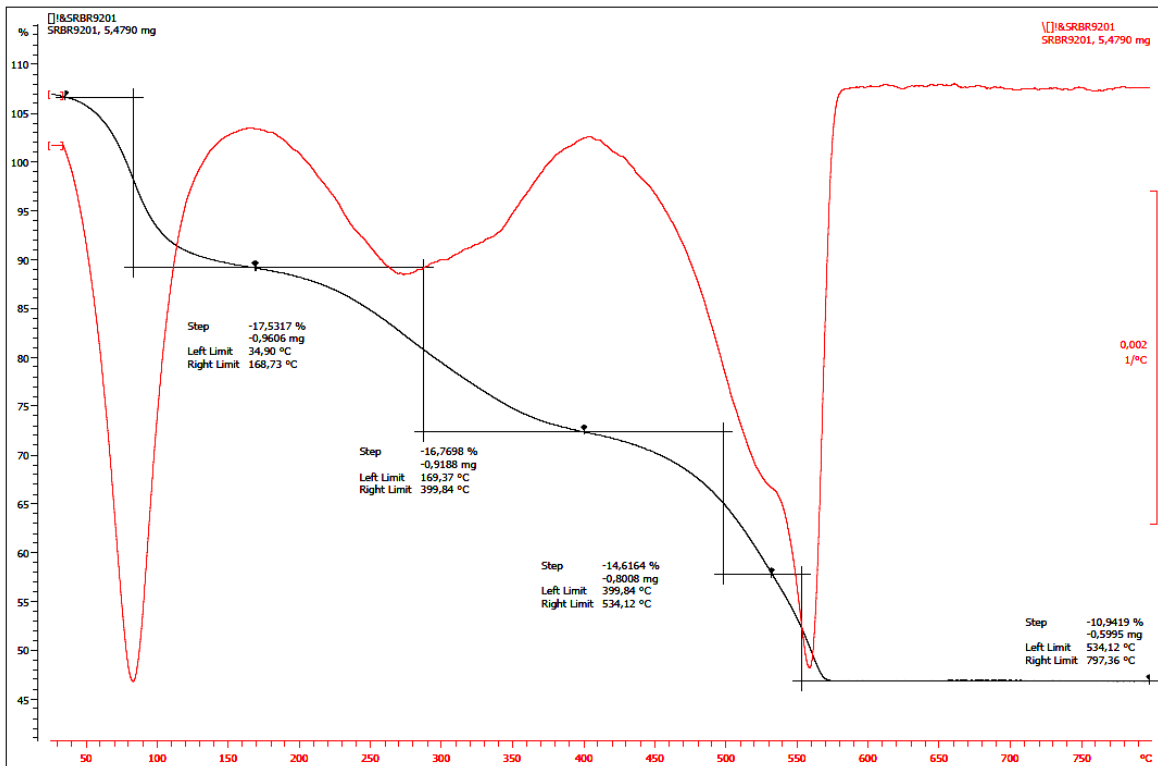


**Figure S20.** TGA and DTA curves of Zr-MOF-808 sample.

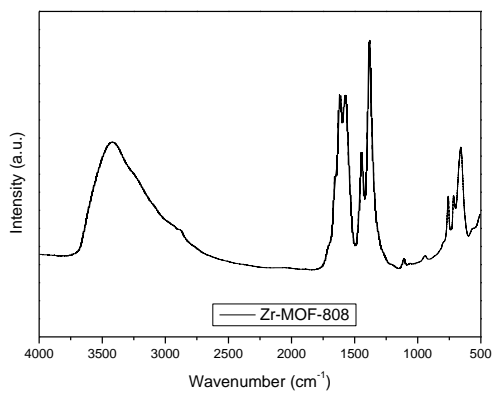


**Figure S21.** FTIR spectrum of Zr-MOF-808 sample

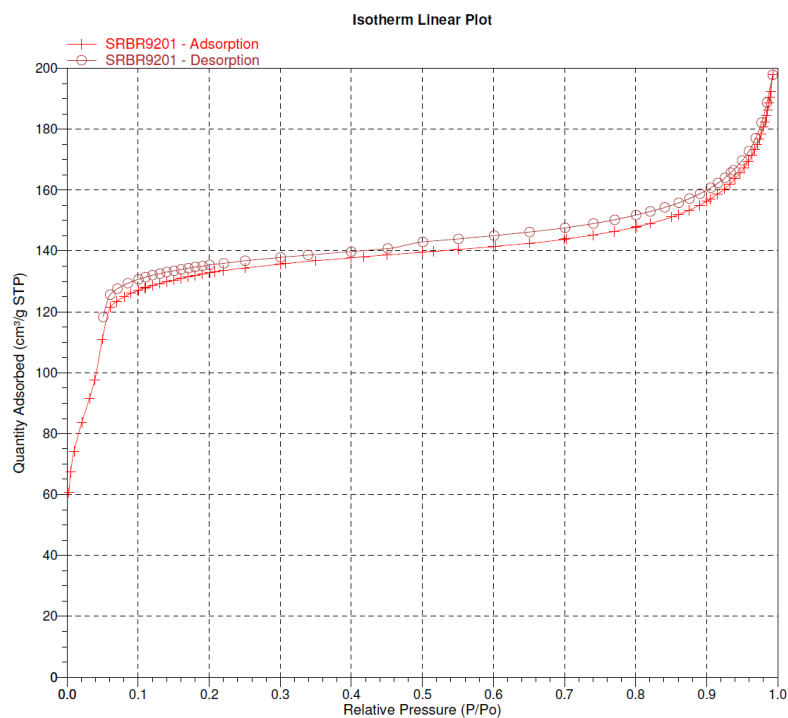


**Figure S22.** N<sub>2</sub> adsorption and desorption isotherm of Zr-MOF-808 sample

**Table S11.** Textural Characteristic of Zr-MOF-808.

Sample	BET Surface Area/m <sup>2</sup> g <sup>-1</sup>	Total Pore Volume/cm <sup>3</sup> g <sup>-1</sup>
Zr-MOF-808	431	0.28

### 1.7. Characterization of the basicity of Zr and Hf-based MOFs by FTIR with a probe molecule such as $\text{CDCl}_3$ .

The samples were pretreated within the IR cell by heating at 120 °C under vacuum for 1.5 h before the sorption experiments. FTIR spectra were recorded on a Bruker Vertex 70 spectrometer in the wavenumber range between 400 and 4000  $\text{cm}^{-1}$  with a resolution of 4  $\text{cm}^{-1}$ .

For the analysis of the basicity, the samples were exposed to  $\text{CDCl}_3$  as probe molecule.  $\text{CDCl}_3$  is a soft probe molecule for basic sites such as amines, ketones, oxides, etc. Difference FTIR spectra of  $\text{CDCl}_3$  adsorbed on Zr and Hf MOF-808 materials, and on Zr and Hf UiO-66 solids are shown below. Two bands (2278 and 2253  $\text{cm}^{-1}$ ) can be disclosed after deconvolution for the UiO-66 solids which evidence the presence to two different basic sites. One band is observed for the MOF-808 materials at 2253  $\text{cm}^{-1}$ . We can conclude from these experiments that these four MOFs show basic sites that could participate in the catalytic procedure. The band at 2253  $\text{cm}^{-1}$  can be assigned to the interactions between  $\text{CDCl}_3$  and the basic sites, which are formed by the carboxylate groups in the framework of UiO-66<sup>[3]</sup> and MOF-808.

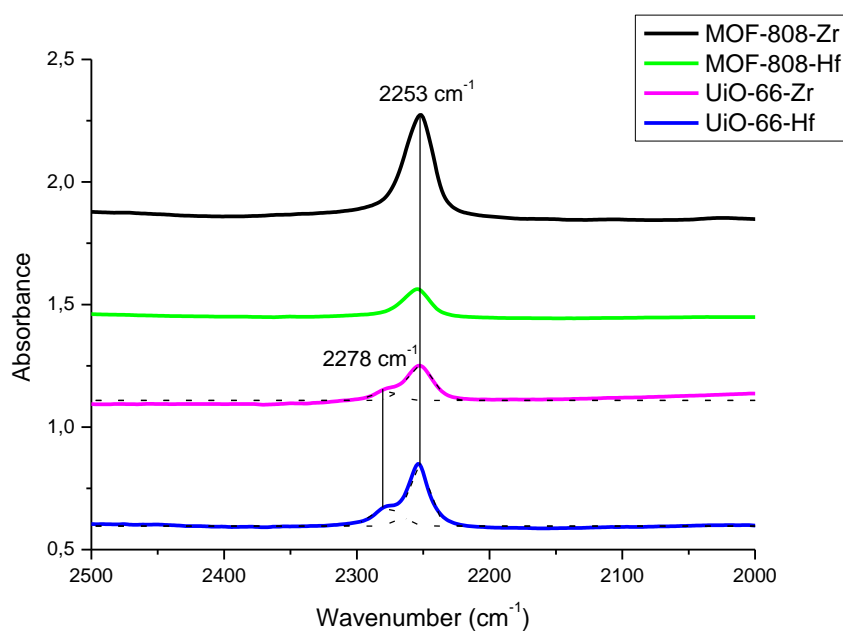


**Figure S23.** FTIR difference spectra of adsorbed  $\text{CDCl}_3$  on various Zr- and Hf-MOFs.

## 1.8. Characterization of the acidity of Zr and Hf-based MOFs by FTIR with a probe molecule such as CD<sub>3</sub>CN.

The samples were pretreated within the IR cell by heating at 120 °C under vacuum for 1.5 h before the sorption experiments. FTIR spectra were recorded on a Bruker Vertex 70 spectrometer in the wavenumber range between 400 and 4000 cm<sup>-1</sup> with a resolution of 4 cm<sup>-1</sup>. The samples were exposed to CD<sub>3</sub>CN. Difference FTIR spectra are shown below. For Zr- and Hf-MOF-808 materials (Figure S24A), two bands are clearly observed. The one at 2261 cm<sup>-1</sup> corresponds to physisorbed molecules. Vibration frequency of chemisorbed CD<sub>3</sub>CN molecules on Lewis acid sites appeared at 2302 and 2305 cm<sup>-1</sup> for MOF-808-Zr and MOF-808-Hf, respectively. The higher shift of the later band for MOF-808-Hf accounts for superior Lewis acidity compared with the related zirconium-based MOF.

In the case of Zr and Hf UiO-66 materials (Figure S24B), two bands are clearly observed. The one at 2260 cm<sup>-1</sup> corresponds to physisorbed molecules. Vibration frequency of chemisorbed CD<sub>3</sub>CN molecules on Lewis acid sites appeared at 2298 and 2302 cm<sup>-1</sup> for UiO-66-Zr and UiO-66-Hf, respectively. The higher shift of the later band for UiO-66-Hf accounts for superior Lewis acidity compared with the related zirconium-based MOF.

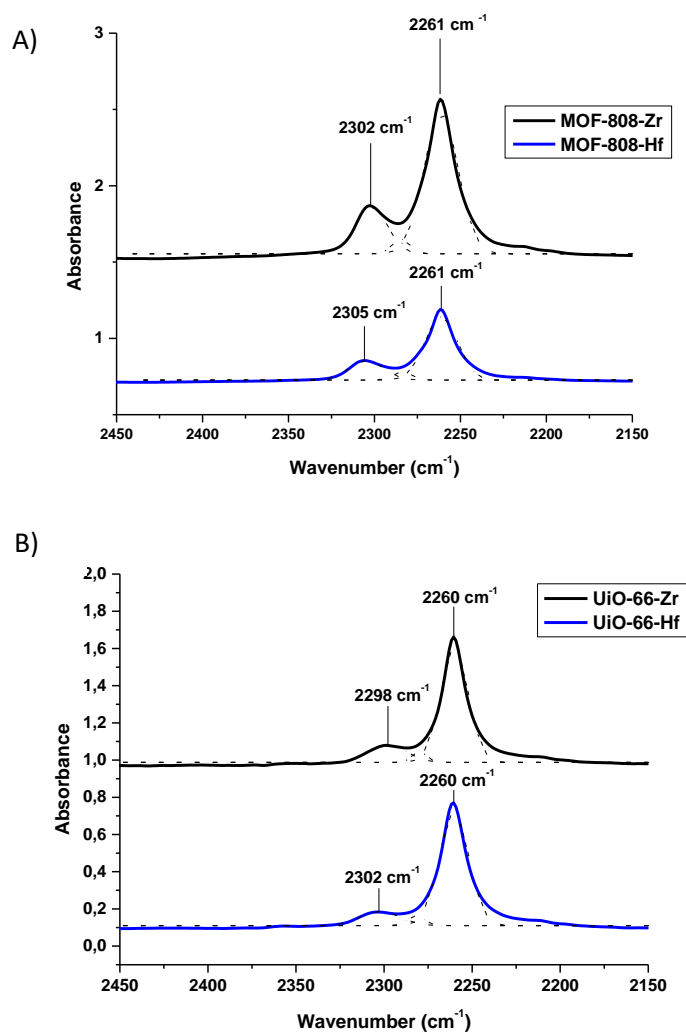


**Figure S24.** A) FTIR difference spectra of adsorbed CD<sub>3</sub>CN on Zr and Hf MOF-808. B) FTIR difference spectra of adsorbed CD<sub>3</sub>CN on Zr and Hf MOF, UiO-66

## 2. Hafnium and zirconium catalysts for the aldol condensation of furfural with acetone.

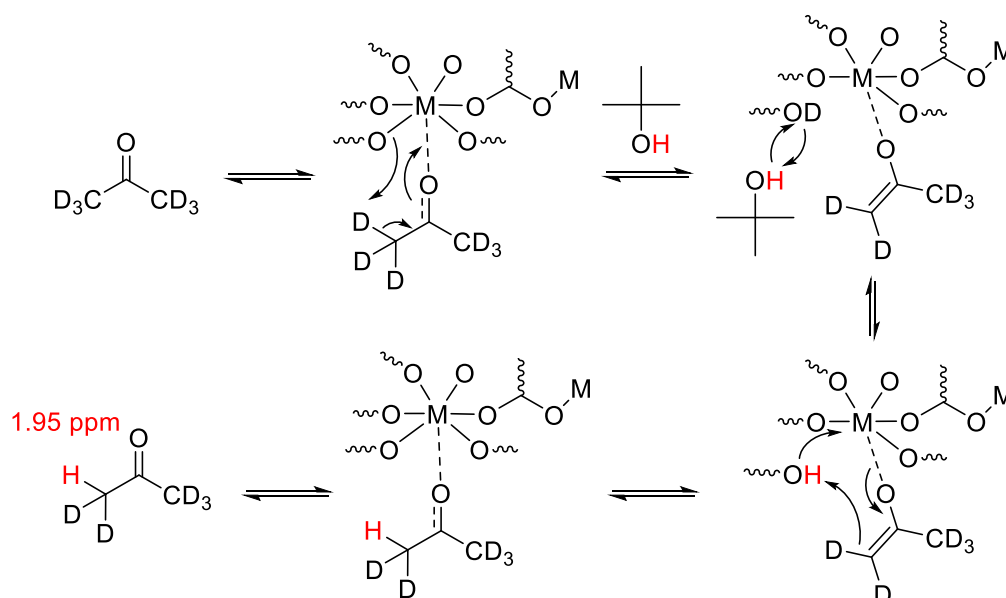
Catalyst screening: Furfural (0.1 mmol, 9.6 mg), catalyst (10 mol % in metal), dodecane (10  $\mu$ L) as internal standard and acetone (0.5 mL) were added to a 1.5 mL glass vessel. The reaction mixture was left to stir at 100  $^{\circ}$ C. The yield was determined by analysis by gas chromatography of aliquots taken from the reaction mixture at different times.

**Table S12.** Calculated TONs and TOFs of the hafnium- and zirconium-based MOFs, for the aldol condensation of furfural with acetone. TOFs were calculated at initial reaction rate as moles of product formed per hour and per mole of metal site.

Catalyst	TON	TOF ( $\text{h}^{-1}$ )
UiO-66(Hf)	9,8	9,7
Hf-MOF-808	9,3	5,2
Zr-MOF-808	9,3	4,8
UiO-66(Zr)	7,7	1,7
UiO-66-NH <sub>2</sub> (Hf)	7,5	1,5
HfCl <sub>4</sub>	4,4	1,3
UiO-67(Hf)	2,5	0,6

## 3. Mechanistic studies using NMR spectroscopy and deuterated acetone.

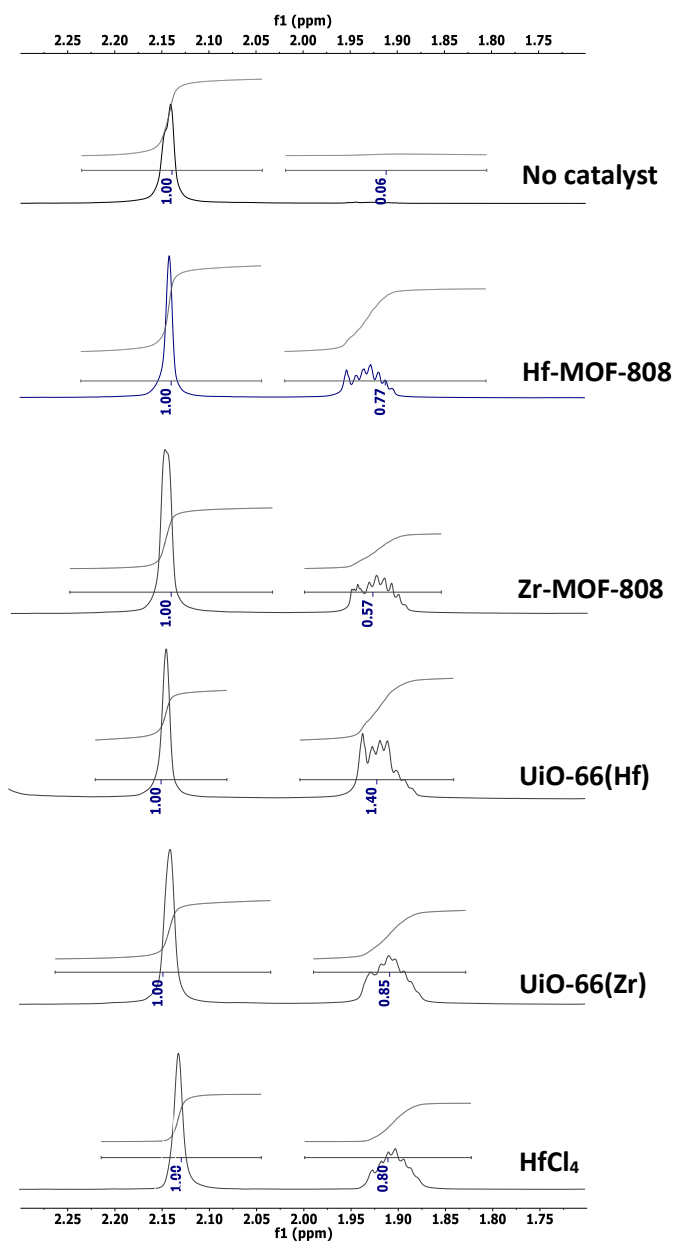
Enolate formation study: Solutions for the enolate study were prepared with 70  $\mu$ L  $d_6$ -acetone in 0.43 mL of *t*BuOH. Toluene was added as an internal standard (10  $\mu$ L). Catalyst was added such that (mmol acetone)/(mmol Hf or Zr)= 95:1. The mixture was left stir at 100  $^{\circ}$ C for 6 hours. Solid was removed and the liquid phase was analyzed by  $^1\text{H}$  NMR in  $\text{CDCl}_3$ .



**Scheme S1.** Mechanistic pathway of acetone enolate formation at Hf- and Zr-MOF active site.

**Table S13.** Ratio of  $\alpha$ -protons in acetone: methyl signal in toluene (as internal standard) measured by  $^1\text{H}$  NMR spectroscopy using different catalysts.

Catalyst	$\alpha$ -H acetone:Toluene
-	0.06
Hf-MOF-808	0.77
Zr-MOF-808	0.57
UiO-66(Hf)	1.40
UiO-66(Zr)	0.85
$\text{HfCl}_4$	0.80



#### 4. Hf-MOFs tolerance to various contaminants in the aldol condensation of furfural with acetone.

Blank experiment: Furfural (0.1 mmol, 9.6 mg), catalyst (10 mol % in metal), dodecane (10  $\mu$ L) as internal standard and acetone (0.5 mL) were added to a 1.5 mL glass vessel. The reaction mixture was left to stir at 100  $^{\circ}$ C. The yield was determined by analysis by gas chromatography of aliquots taken from the reaction mixture at different times.

Water as contaminant: Furfural (0.1 mmol, 9.6 mg), catalyst (10 mol % in metal), dodecane (10  $\mu$ L) as internal standard, acetone (0.5 mL) and water (100 mg, 100  $\mu$ L) were added to a 1.5 mL glass vessel. The reaction mixture was left to stir at 100  $^{\circ}$ C. The yield was determined by analysis by gas chromatography of aliquots taken from the reaction mixture at different times.

Acetic acid as contaminant: Furfural (0.1 mmol, 9.6 mg), catalyst (10 mol % in metal), dodecane (10  $\mu$ L) as internal standard and a stock solution (0.08 M) of acetic acid in acetone (0.5 mL) were added to a 1.5 mL glass vessel. The reaction mixture was left to stir at 100  $^{\circ}$ C. The yield was determined by analysis by gas chromatography of aliquots taken from the reaction mixture at different times.

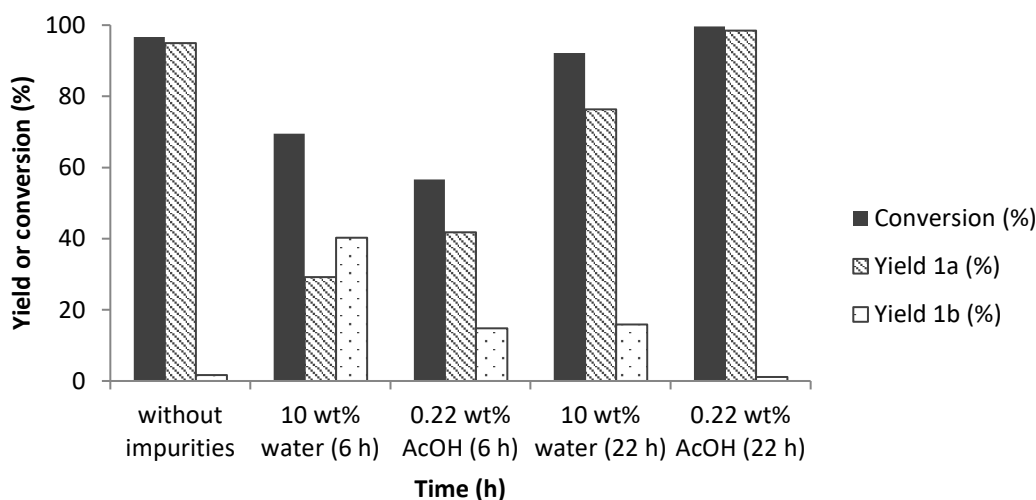
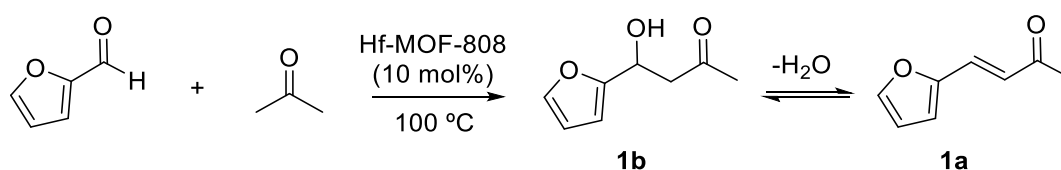
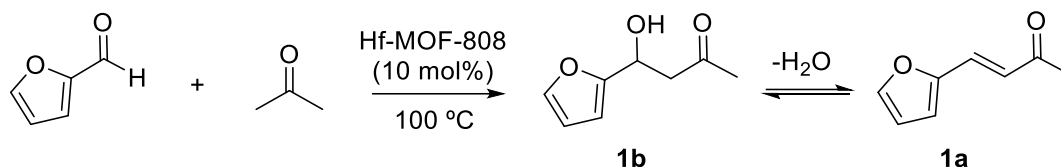


**Figure S25.** Effects of water and acetic acid on the aldol condensation of furfural and acetone with catalyst MOF-808-Hf. Reaction Conditions: 0.1 mmol furfural, catalyst (10 mol%), dodecane (10  $\mu$ L) as internal standard, acetone (0.5 mL), T = 100 $^{\circ}$ C. Water (10 wt% with 600:10:1 water:substrate:Hf molar ratio) was also added. Acetic acid (0.22 wt% with 4:10:1 acetic acid:substrate:Hf molar ratio) was also added.

## 5. Stability and reuses of Hf-MOF-808. Characterization of Hf-MOF-808 material after repeated utilization.



Filtration test in the aldol condensation of furfural with acetone: Furfural (0.1 mmol, 9.6 mg), catalyst (10 mol % in metal), dodecane (10  $\mu$ L) as internal standard and acetone (0.5 mL) were added to a 1.5 mL glass vessel. The reaction mixture was left to stir at 100 °C. The solid was filtered off after 30 min reaction time and the filtrate was left to stir further at 100°C. The yield was determined by analysis by gas chromatography of aliquots taken from the reaction mixture at different times.

Reuse study in the aldol condensation of furfural with acetone: Furfural (0.5 mmol, 48 mg), catalyst (10 mol % in metal), dodecane (40  $\mu$ L) as internal standard and acetone (2.5 mL) were added to a 10 mL pyrex glass tube. The reaction mixture was left to stir at 100 °C for 6 hours. The yield was determined by analysis by gas chromatography. The solid catalyst was then separated by centrifugation and then washed with EtOAc and acetone. The catalyst was activated in *vacuo* for 2 h at room temperature and then used for the next run. In the soxhlet experiment, after the third run, the catalyst was extracted in a soxhlet with ethyl acetate for 24 hours. Then, the solid was dried at 100 °C during a night and used in the next run.

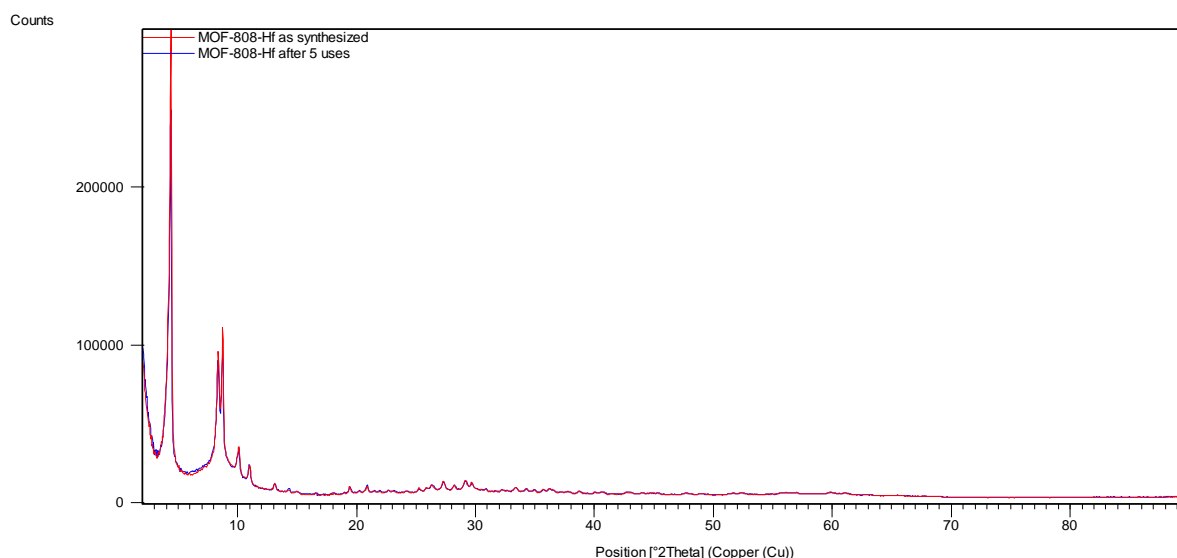


**Figure S26.** XRD pattern of Hf-MOF-808. Red line: as synthesized material. Blue line: Hf-MOF-808 after utilization in 5 consecutive runs.

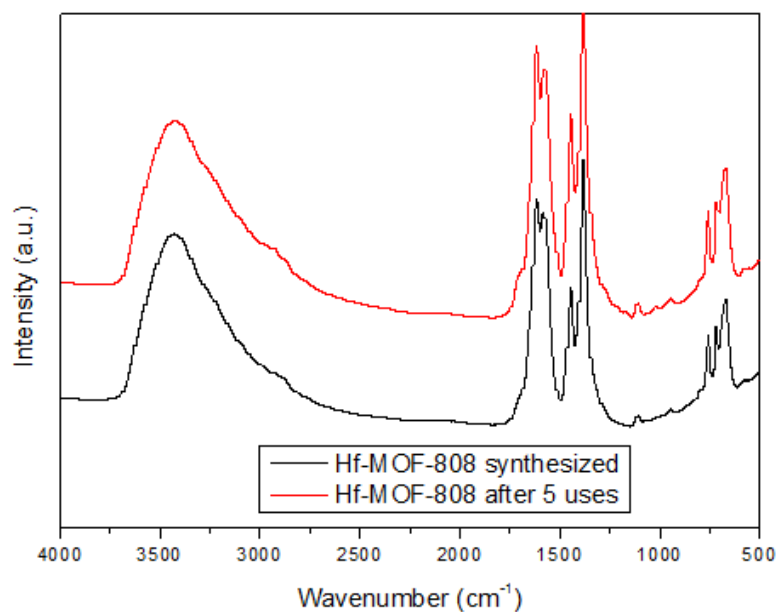


**Figure S27.** FTIR spectrum of Hf-MOF-808 sample. Red line: as synthesized material. Black line: Hf-MOF-808 after utilization in 5 consecutive runs.

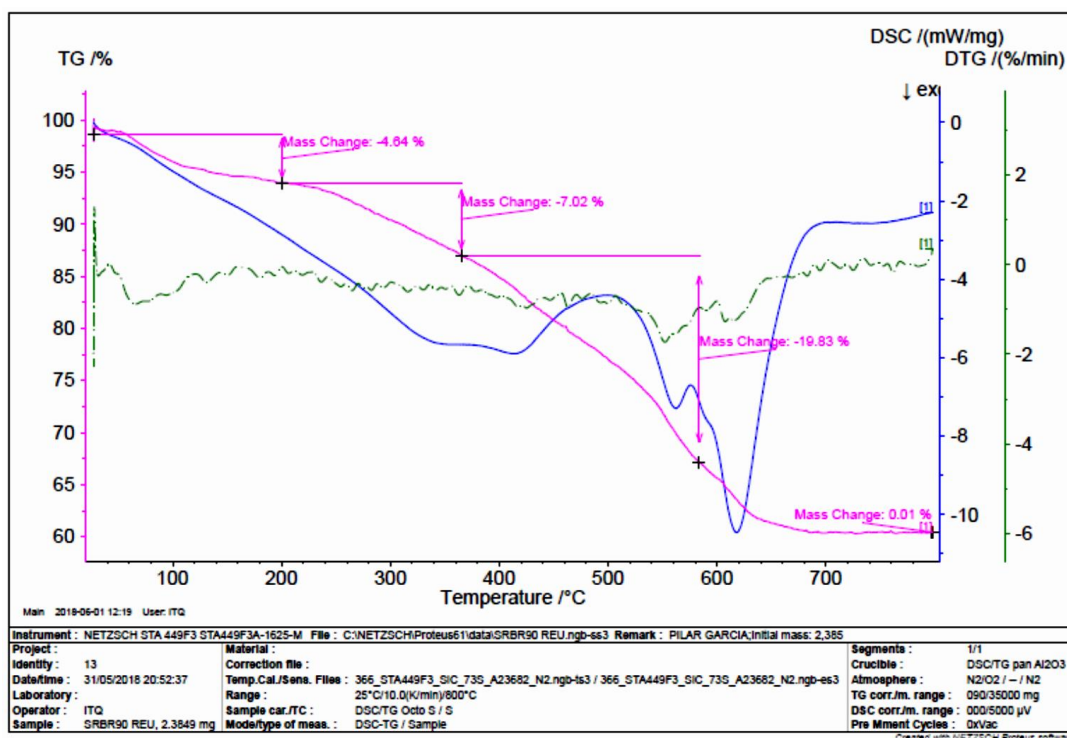


**Figure S.** TGA and DTA curves of Hf-MOF-808 after 5 consecutive uses

**Table S14.** Chemical analysis of Hf-MOF-808 sample as synthesized and after utilization in 5 consecutive runs.

Sample	C <sup>a</sup>	H <sup>a</sup>	N <sup>a</sup>	Metal <sup>b</sup>	Org. Cont. <sup>a</sup>	
					CHN <sup>c</sup>	TGA <sup>d</sup>
Hf-MOF-808 as synthesized.	13.9	1.3	0.3	46	15.5	29
Hf-MOF-808 after 5 uses	19.8	1.8	0.8	44	22.4	31.5

<sup>a</sup>Percentage in weight (% wt); <sup>b</sup>Determined by ICP analysis <sup>c</sup>Organic content from CHNS elemental analysis, <sup>d</sup>Organic content from thermogravimetric analysis without taking into account hydration water.

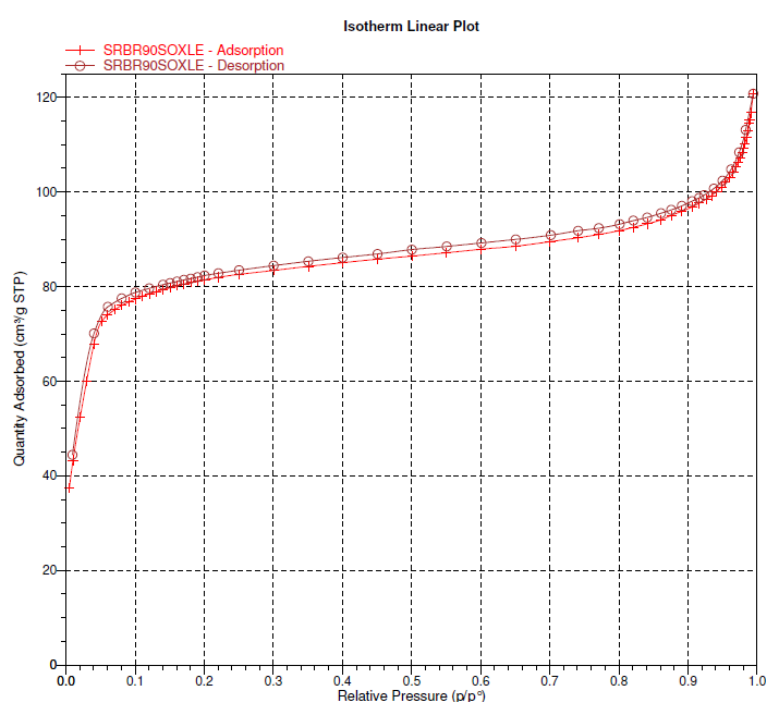
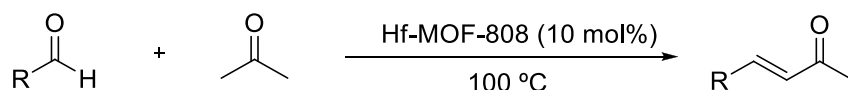


**Figure S28.** N<sub>2</sub> adsorption and desorption isotherm of Hf-MOF-808 sample after 3 uses and soxhlet extraction.

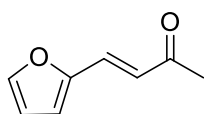
**Table S15.** Textural characteristic of Hf-MOF-808 as synthesized, after 5 uses in the transfer hydrogenation reaction of furfural with isopropanol<sup>[4]</sup> and after 3 uses + soxhlet in the aldol condensation of furfural with acetone.

Sample	BET Surface Area/m <sup>2</sup> g <sup>-1</sup>	Total Pore Volume/cm <sup>3</sup> g <sup>-1</sup>
Hf-MOF-808 as synthesized	458	0.3
Hf-MOF-808 after 5 uses in transfer hydrogenation reaction of furfural <sup>[4]</sup>	35	0.09
Hf-MOF-808 after 3 runs in aldol condensation and Soxhlet extraction	270	0.19

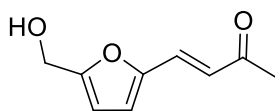
## 6. General procedure for the synthesis of enones.



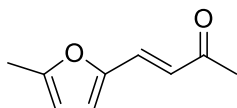
Hf-MOF-808 (20 mg, 0.05 mmol, 10 mol%) was placed in a 10 mL pyrex glass vessel. The vessel can withstand pressure. Aldehyde (0.5 mmol) and acetone (2.5 mL) were then added and the mixture was left to stir vigorously at 100 °C for the corresponding time. The reaction mixture was then filtered in order to separate the catalyst that was washed with ethyl acetate. Solvent was then removed under reduced pressure and the crude product was purified by column chromatography using hexane/ethyl acetate as eluent. All the products obtained have been described previously (reference given below for each of them) and were characterized by GC-MS and NMR spectroscopy.



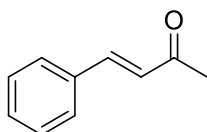
**4-(furan-2-yl)but-3-en-2-one:** The reaction mixture was left for 12 h to give a yellow oil in 92% yield (62.6 mg, 0.46 mmol). **<sup>1</sup>H-NMR (300 MHz, CDCl<sub>3</sub>):**<sup>[5]</sup> δ 7.43 (d, J=1.2 Hz, 1H), 7.21 (d, J=15.9 Hz, 1H), 6.60 (d, J=3.4 Hz, 1H), 6.55 (d, J=15.9 Hz, 1H), 6.42 (dd, J=3.4, 1.8 Hz, 1H), 2.26 (s, 3H).



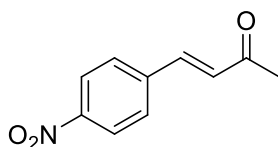
**4-(5-(hydroxymethyl)furan-2-yl)but-3-en-2-one:** The reaction mixture was left for 9 h to give a yellow oil in 91% yield (75.6 mg, 0.45 mmol). **<sup>1</sup>H-NMR (300 MHz, CDCl<sub>3</sub>):**<sup>[6]</sup> δ 7.15 (d, J=15.9 Hz, 1H), 6.54 (d, J=3.3 Hz, 1H), 6.50 (d, J=15.9 Hz, 1H), 6.30 (d, J=3.3 Hz, 1H), 4.56 (s, 2H), 2.22 (s, 3H).



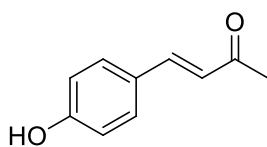
**4-(5-(methylfuran-2-yl)but-3-en-2-one:** The reaction mixture was left for 24 h to give a yellow oil in 89% yield (66.8 mg, 0.44 mmol).  $^1\text{H-NMR}$  (300 MHz,  $\text{CDCl}_3$ ):  $\delta$  7.14 (d,  $J=15.8$  Hz, 1H), 6.50 (d,  $J=3.2$  Hz, 1H), 6.47 (d,  $J=15.7$  Hz, 1H), 6.03 (d,  $J=3.2$  Hz, 1H), 2.28 (s, 3H), 2.24 (s, 3H).



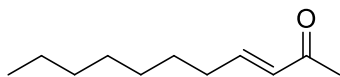
**4-phenylbut-3-en-2-one:** The reaction mixture was left for 24 h to give a white solid in 94% yield (68.7 mg, 0.47 mmol).  $^1\text{H-NMR}$  (300 MHz,  $\text{CDCl}_3$ ):<sup>[7]</sup>  $\delta$  7.49-7.46 (m, 2H), 7.43 (d,  $J = 15.9$  Hz, 1H), 7.33-7.31 (m, 3H), 6.65 (d,  $J=16.3$  Hz, 1H), 2.31 (s, 3H).



**4-(4-nitrophenyl)but-3-en-2-one:** The reaction mixture was left for 3 h to give a yellow solid in 92% yield (87.9, 0.46 mmol).  $^1\text{H-NMR}$  (300 MHz,  $\text{CDCl}_3$ ):<sup>[8]</sup>  $\delta$  8.18 (d,  $J=8.6$ , 2H), 7.63 (d,  $J=8.6$  Hz, 2H), 7.46 (d,  $J=16.2$  Hz, 1H), 6.75 (d,  $J=16.2$  Hz, 1H), 2.35 (s, 3H).



**4-(4-hydroxyphenyl)but-3-en-2-one:** The reaction mixture was left for 36 h to give a yellow solid in 89% yield (72.2 mg, 0.44 mmol).  $^1\text{H-NMR}$  (300 MHz,  $\text{CDCl}_3$ ):<sup>[9]</sup>  $\delta$  7.66 (brs, 1H), 7.45 (d,  $J = 16.5$  Hz, 1H), 7.37 (d,  $J = 8.6$  Hz, 2H), 6.84 (d,  $J=8.6$  Hz, 2H), 6.54 (d,  $J=16.5$  Hz, 1H), 2.32 (s, 3H).  $^{13}\text{C-NMR}$  (75 MHz,  $\text{CDCl}_3$ ):  $\delta$  200.2, 159.1, 144.9, 130.5, 126.4, 124.3, 116.2, 27.2.



**Undec-3-en-2-one:** The reaction mixture was left for 48 h to give a yellow oil in 93% yield (78.2 mg, 0.47 mmol). <sup>1</sup>H-NMR (300 MHz, CDCl<sub>3</sub>): δ 6.73 (dt, J = 6.7 and 15.0 Hz, 1H), 5.99 (d, 15.0 Hz, 1H), 2.17 (s, 3H), 2.16-2.11 (m, 2H), 1.41-1.35 (m, 2H), 1.21 (m, 8H), 0.81 (t, 6.5 Hz, 3H).

### 7. Two-step one-pot transformation of benzaldehyde to 4-phenyl-3-buten-2-ol.

Benzaldehyde (0.1 mmol, 10.6 mg), Hf-MOF-808 (10 mol%), dodecane (10 μL) as internal standard and acetone (0.5 mL) were added to a 1.5 mL glass vessel. The reaction mixture was left to stir at 100 °C for 22 hours. The yield was determined by analysis by gas chromatography of aliquots taken from the reaction mixture at different times to get the kinetic curve shown below. The aldol reaction was run in a duplicated manner, to use one of the experiments in the drawing of the kinetic curve and the other one to be used in the one-pot procedure. In the latter, solvent was then evaporated in *vacuo*. 2-propanol (0.4 mL) and dodecane (10 μL) as internal standard (not used before) were then added and the reaction mixture further stirred at 120 °C. Yield was determined by analysis by gas chromatography of aliquots taken from the reaction mixture at different times.

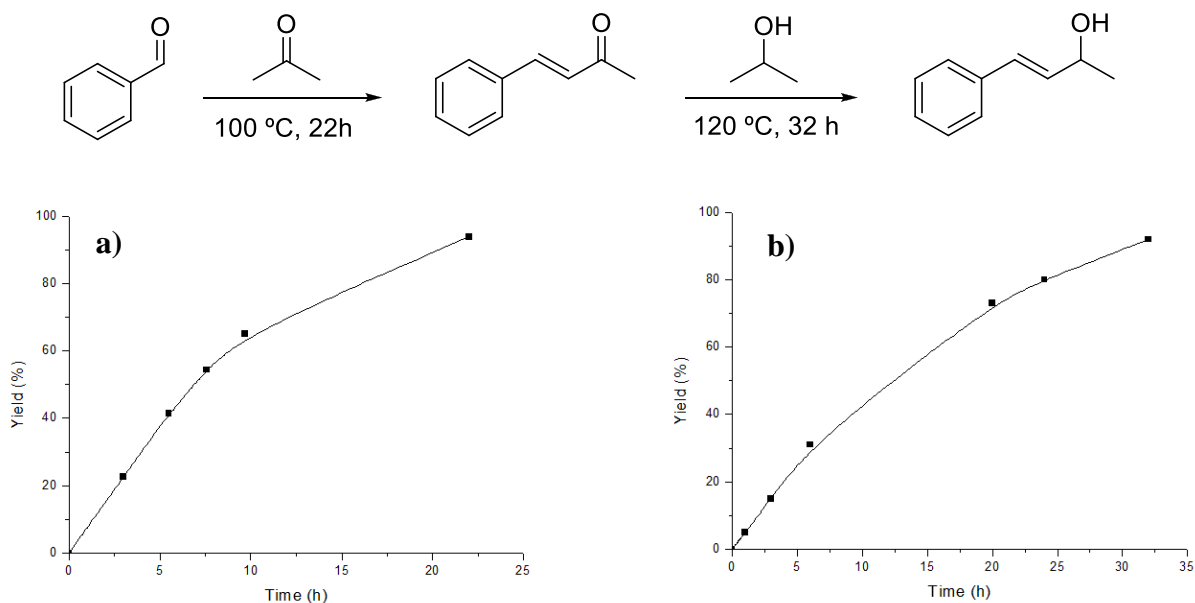


**Figure S29.** Kinetic plots of each step in the one-pot tandem transformation of benzaldehyde to 4-phenyl-3-buten-2-ol. a) aldol condensation between benzaldehyde and acetone to give 4-phenyl-3-buten-2-one. b) Meerwein-Ponndorf Verley reduction of the latter using isopropanol as reduction agent to yield 4-phenyl-3-buten-2-ol.

## 8. Synthesis and catalytic activity of Pd@Hf-MOF-808:

Synthesis and characterization of Pd@Hf-MOF-808: A mixture of HfCl<sub>4</sub> (160 mg, 0.5 mmol), 1,3,5,-benzenetricarboxylic acid (110 mg, 0.5 mmol), palladium acetate (2.5 mg, 0.01 mmol), dimethylformamide /formic acid (20 mL:20 mL) was sonicated for 30 min and then added to an autoclave vessel and heated at 100 °C for 72 h. The resulting solid was filtered and washed with an excess of DMF and acetone. The as-synthesized solid was activated at 120 °C in *vacuo* for 12 h. The powder X-ray diffraction pattern showed that the solid material has the crystal structure as MOF-808 type solids. ICP analysis shows 49% Hf and 1.2% Pd.

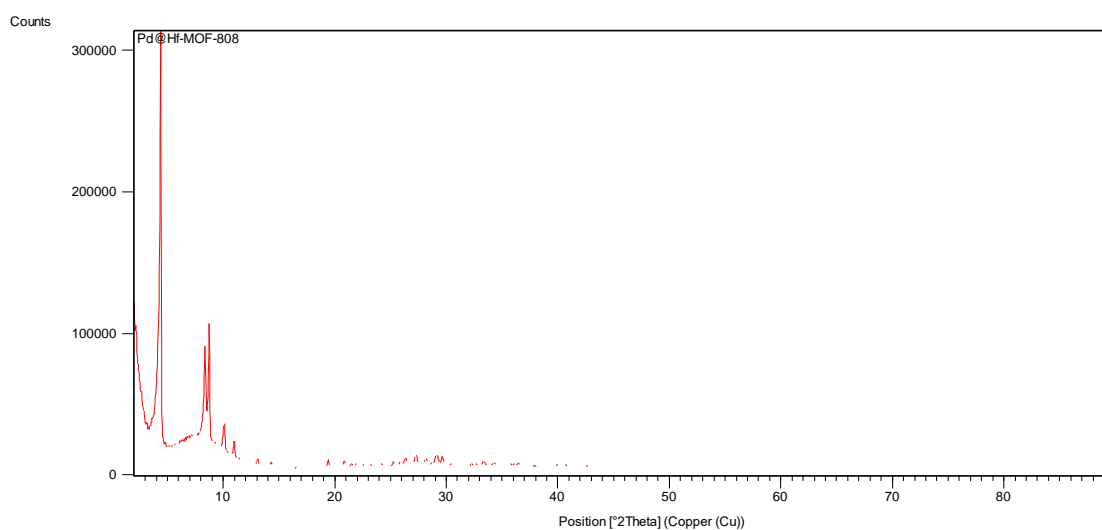


**Figure S30.** XRD pattern of Pd@Hf-MOF-808

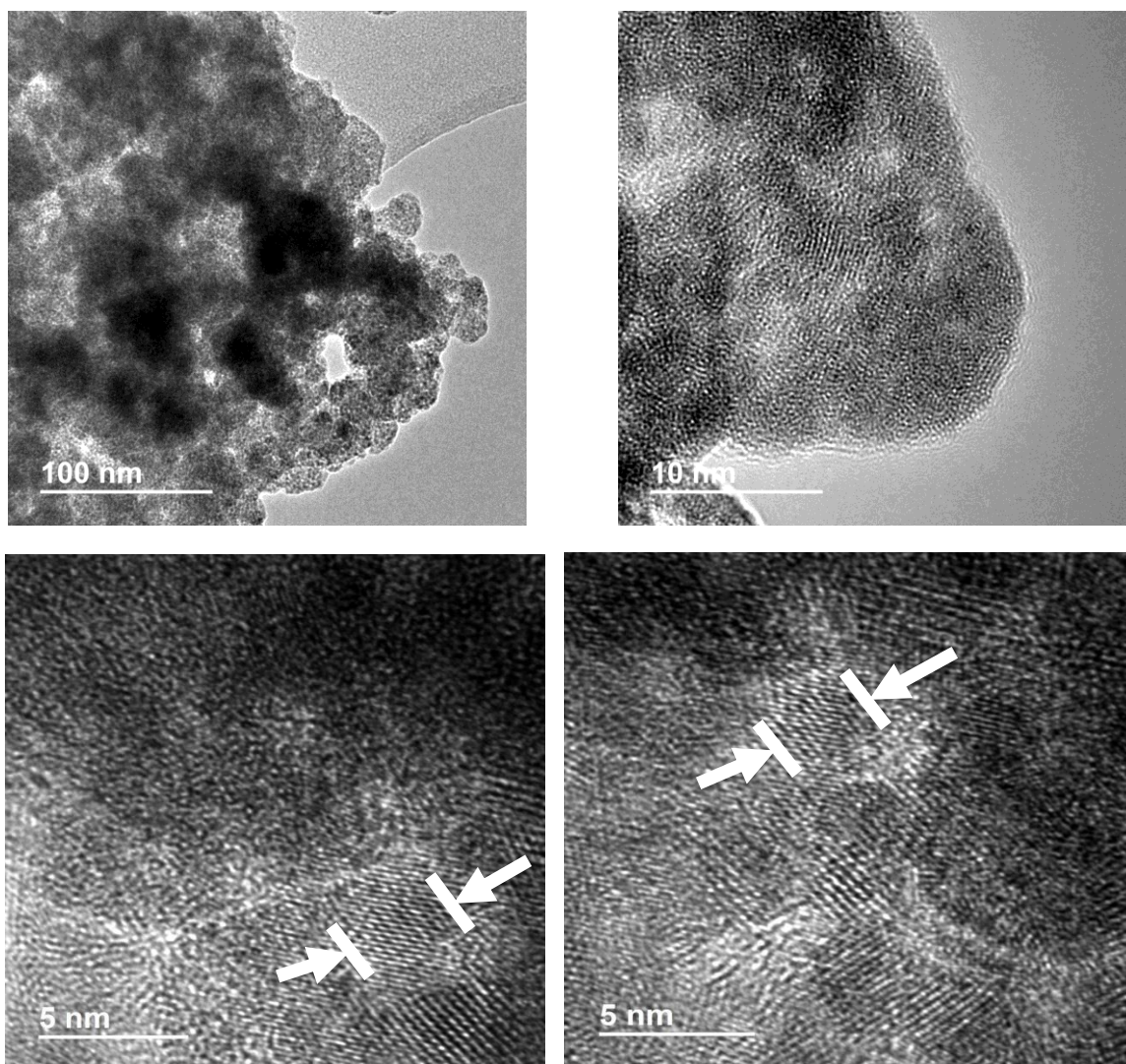


**Figure S31.** HRTEM images of Pd@Hf-MOF-808. Scale bars are included in each micrograph.

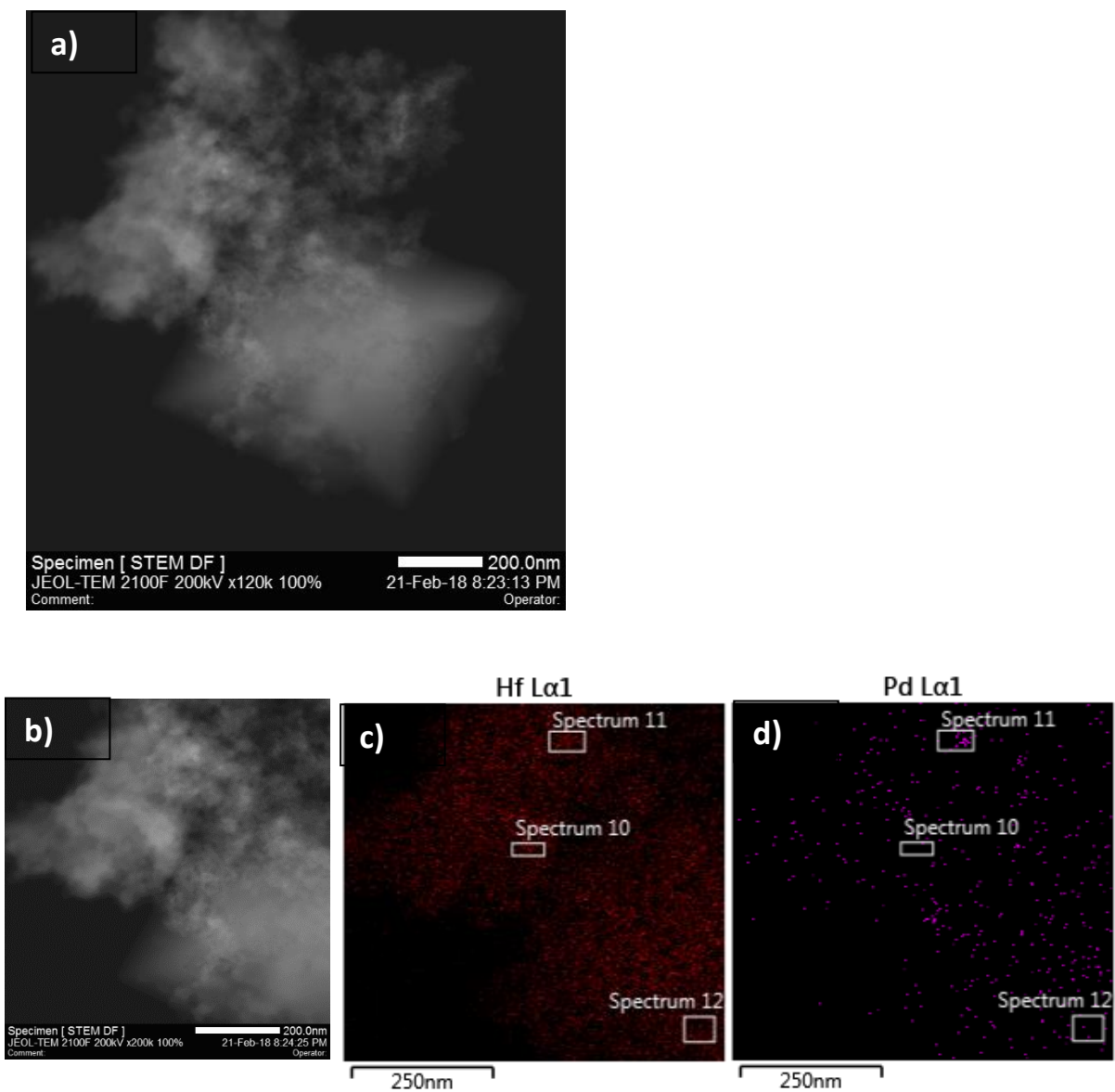


**Figure S32.** STEM images a) and b) of Pd@Hf-MOF-808. a) octahedral crystal of Hf-MOF-808 with surrounding amorphous solid. b) is part of image a). c) and d) show elemental mappings for Hf and Pd respectively. Spectrum 11 is the zone that shows appreciable amount of palladium.

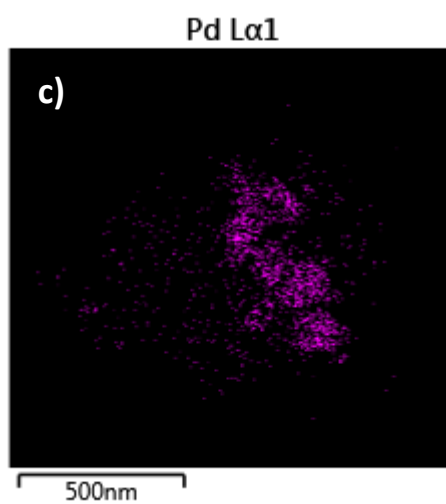
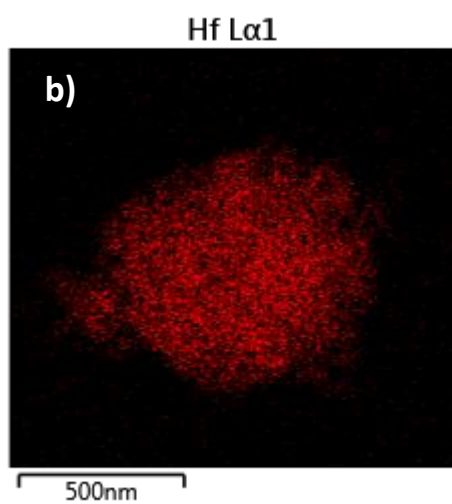
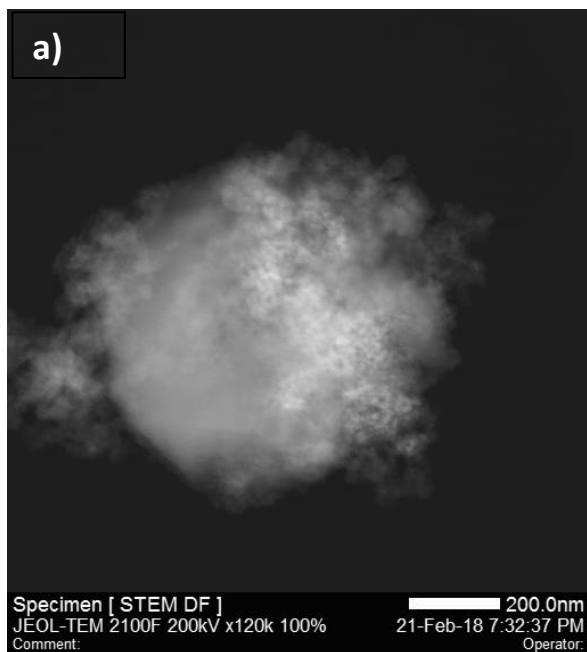


**Figure S33.** a) STEM image of Pd@Hf-MOF-808. Octahedral crystal of Hf-MOF-808 is shown with surrounding amorphous solid. b) and c) show elemental mappings for Hf and Pd respectively.

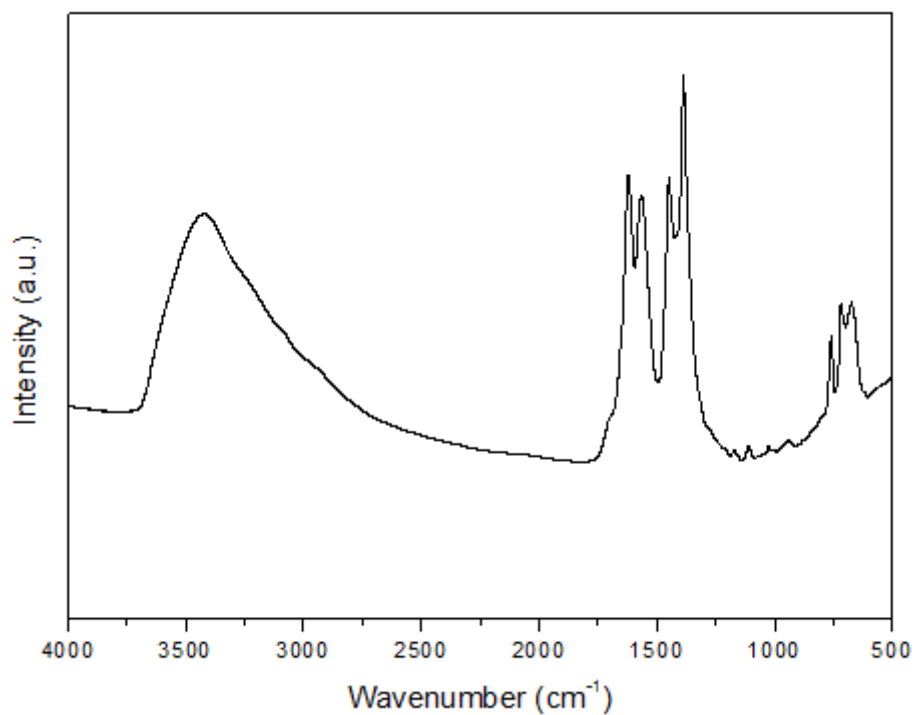


**Figure S34.** FTIR spectrum of Pd@Hf-MOF-808 sample.

**Table S16.** Chemical analysis of Pd@Hf-MOF-808 sample.

Sample	C <sup>a</sup>	H <sup>a</sup>	N <sup>a</sup>	Hf <sup>b</sup>	Pd <sup>b</sup>	Org. Cont. <sup>a</sup>
						CHN <sup>c</sup>
Pd@Hf-MOF-808	14.6	1.9	0.9	49	1.2	17.4

<sup>a</sup> Percentage in weight (%wt); <sup>b</sup> Determined by ICP analysis <sup>c</sup> Organic content from CHNS elemental analysis.

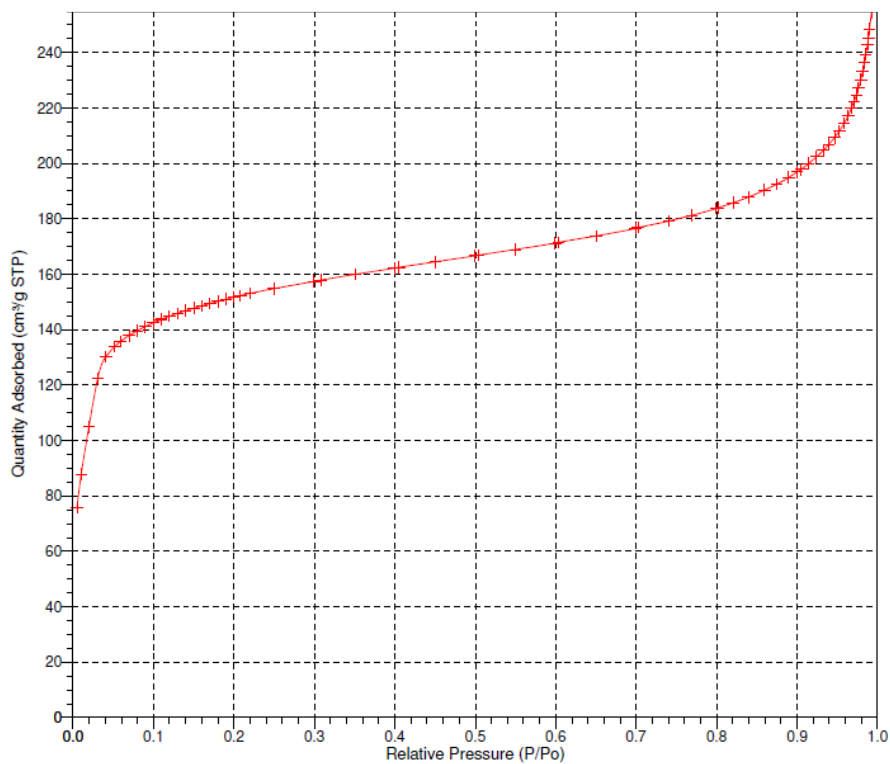
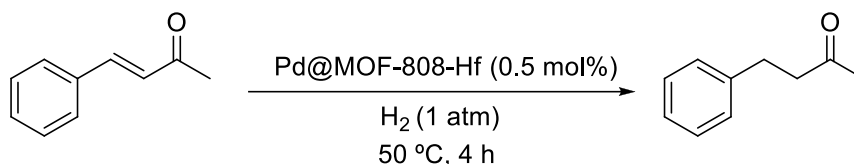


**Figure S35.** N<sub>2</sub> adsorption isotherm of Pd@Hf-MOF-808 sample

**Table S17.** Textural Characteristic of Pd@Hf-MOF-808

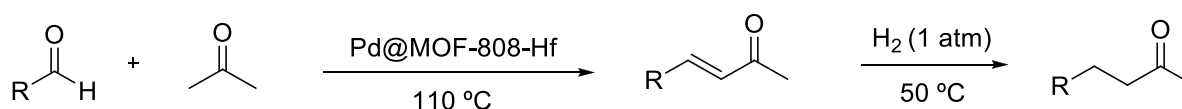
Sample	BET Surface Area/m <sup>2</sup> g <sup>-1</sup>	Total Pore Volume/cm <sup>3</sup> g <sup>-1</sup>
<b>Pd@Hf-MOF-808</b>	<b>500</b>	<b>0.39</b>

### Pd@Hf-MOF-808 in the hydrogenation reaction of enones

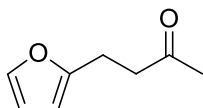


4-phenylbut-3-en-2-one (0.5 mmol, 73 mg), Pd@MOF-808-Hf (25 mg,  $2.5 \times 10^{-3}$  mmol, 0.5 mol% in Pd), dodecane (40  $\mu$ L) as internal standard and acetone (2.5 mL) were added to a 10 mL glass vessel. The vessel was sealed and purged with H<sub>2</sub> balloon (1 atm). The reaction mixture was then left to stir at 50 °C for 4 hours. Yield was determined by analysis by gas chromatography. The product was isolated at the end of the reaction by column chromatography (70.4 mg, 0.48 mmol, 95%).

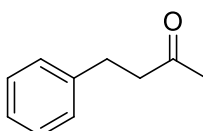
### Pd@Hf-MOF-808 in the two-step one-pot transformation of aldehydes to 4-aryl-butan-2-ones



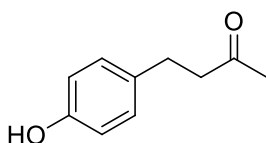
Aldehyde (0.5 mmol), Pd@MOF-808-Hf (25 mg, 14 mol% Hf, 0.5 mol% Pd), dodecane (50  $\mu$ L) and acetone (2.5 mL) were added to a 10 mL pyrex glass vessel. The vessel can withstand pressure. The reaction mixture was left to stir at 110 °C for the corresponding time and analyzed by gas chromatography. When the first step was completed, the vessel was purged with H<sub>2</sub> balloon (1 atm) and the reaction mixture was left to stir at 50 °C for the corresponding time. The solid was then filtered and the catalyst washed with ethyl acetate. Solvent was then removed under reduced pressure and the crude product was purified by column chromatography using hexane/ethyl acetate as eluent. All the products obtained here have been described previously and were characterized by GC-MS and NMR spectroscopy.



**4-(furan-2-yl)butan-2-one:** The aldol condensation reaction was left for 4 h and the hydrogenation was left for 4 h. The product was isolated in 85% yield (58 mg, 0.42 mmol). **<sup>1</sup>H-NMR (300 MHz, CDCl<sub>3</sub>):**<sup>[5]</sup>  $\delta$  7.22 (m, 1H), 6.2 (d, J=2.3 Hz, 1H), 5.92 (d, J=2.9 Hz, 1H), 2.88-2.82 (m, 2H), 2.73-2.69 (m, 2H), 2.09 (s, 3H).

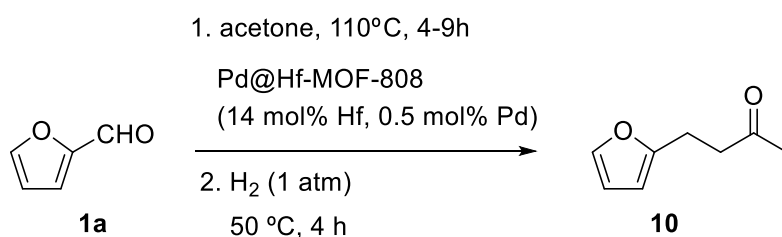


**4-phenylbutan-2-one:** The aldol condensation reaction was left for 12 h and the hydrogenation was left for 4 h. The product was isolated in 90% yield (66.7 mg, 0.45 mmol). **<sup>1</sup>H-NMR (300 MHz, CDCl<sub>3</sub>):**<sup>[5]</sup>  $\delta$  7.23-7.18 (m, 2H), 7.13-7.09 (m, 3H), 2.82 (t, J=7.4 Hz, 2H), 2.68 (t, 7.2 Hz, 2H), 2.06 (s, 3H).



**4-(4-hydroxyphenyl)butan-2-one:** The aldol condensation reaction was left for 12 h and the hydrogenation was left for 4 h. The product was isolated in 82% yield (67.3 mg, 0.41 mmol). **<sup>1</sup>H-NMR (300 MHz, CDCl<sub>3</sub>):**<sup>[10]</sup>  $\delta$  6.94 (d, J = 9Hz, 2H), 6.68 (d, J = 9 Hz, 2H), 2.77-2.72 (m, 2H), 2.66-2.63 (m, 2H), 2.06 (s, 3H).

Stability and reuses of Pd@Hf-MOF-808. Characterization of Pd@Hf-MOF-808 material after repeated utilization.



Furfural (0.5 mmol), Pd@MOF-808-Hf (25 mg, 14 mol% Hf, 0.5 mol% Pd), and acetone (2.5 mL) were added to a 10 mL pyrex glass vessel. The vessel can withstand pressure. The

reaction mixture was left to stir at 110 °C for 4 hours after which time the aldol reaction was completed according to analyses by gas chromatography. When the first step was completed, the vessel was purged with H<sub>2</sub> ballon (1 atm) and the reaction mixture was left to stir at 50 °C for 4 hours. The catalyst was then separated by centrifugation and the solid was washed with EtOAc and acetone. The catalyst was activated in *vacuo* at room temperature and used for the next runs. Second run was performed equally. Aldol reaction step required extended time for subsequent runs while hydrogenation step was similar in all five runs. Reaction time of aldol reaction step in run number three: 6 hours; in run number four: 7.5 hours, in run number five: 9 hours.

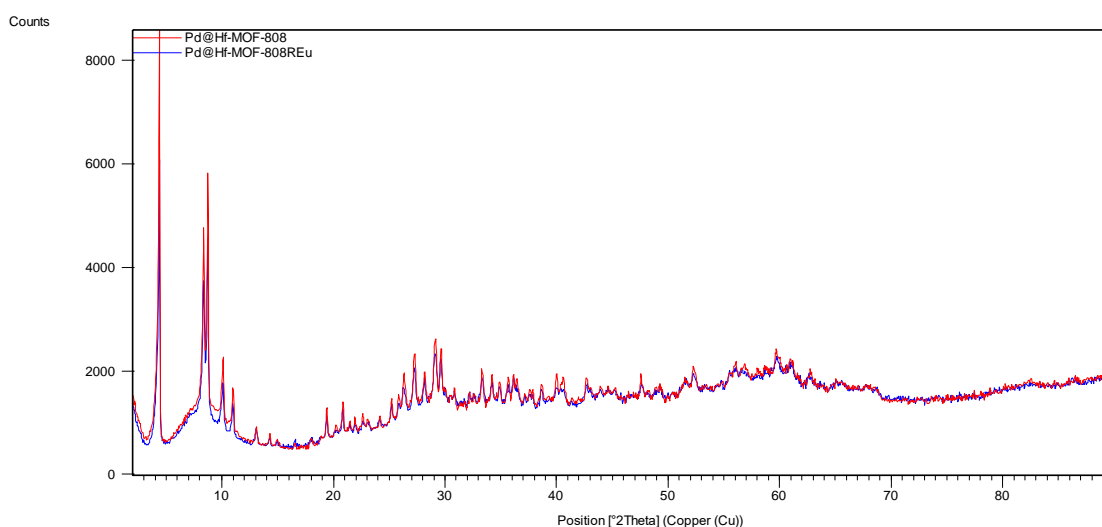


**Figure S36.** XRD pattern of Pd@Hf-MOF-808. Red line: as synthesized material. Blue line: Pd@Hf-MOF-808 after utilization in 5 consecutive runs.

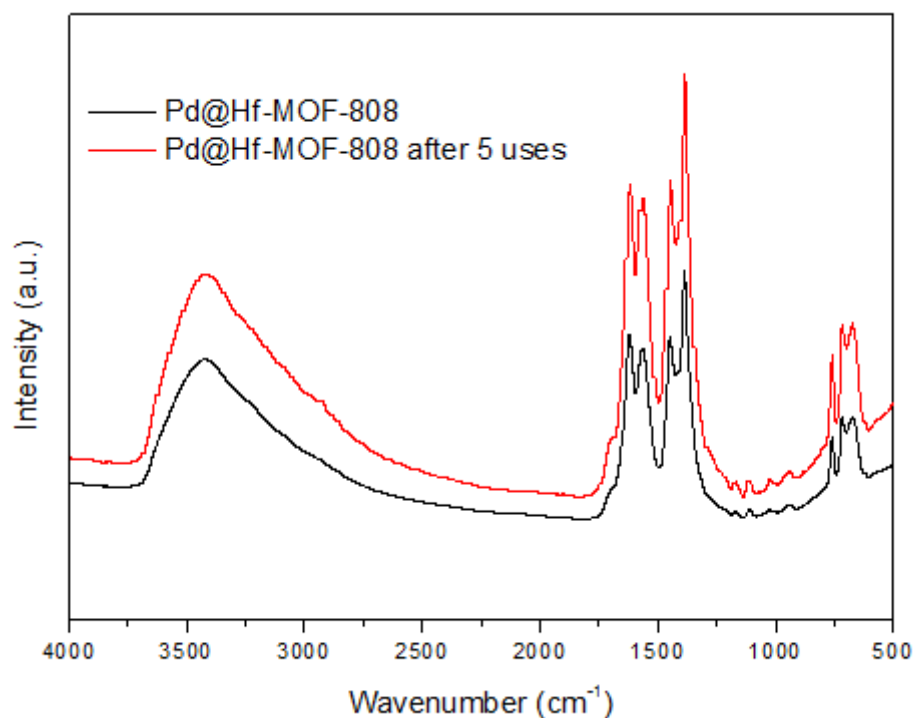


**Figure S37.** FTIR spectra of Pd@ Hf-MOF-808 sample. Black line: as synthesized material. Red line: Pd@Hf-MOF-808 after utilization in 5 consecutive runs.

**Table S18.** Chemical analysis of Pd@Hf-MOF-808 sample as synthesized and after utilization in 5 consecutive runs.

Sample	C <sup>a</sup>	H <sup>a</sup>	N <sup>a</sup>	Hf <sup>b</sup>	Pd <sup>b</sup>	Org. Cont. <sup>a</sup>
						CHN <sup>c</sup>
Pd@Hf-MOF-808 as synthesized	14.6	1.9	0.9	49	1.2	17.4
Pd@Hf-MOF-808 after 5 runs	18.8	1.9	0.3	47	1.1	21.0

<sup>a</sup>Percentage in weight (% wt); <sup>b</sup>Determined by ICP analysis <sup>c</sup>Organic content from CHNS elemental analysis.

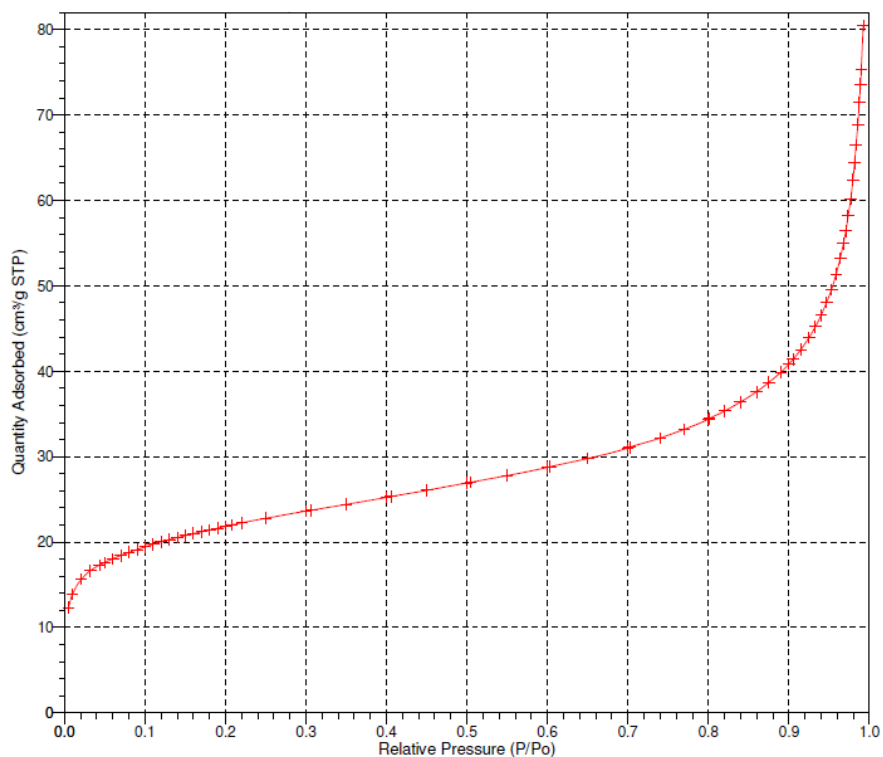
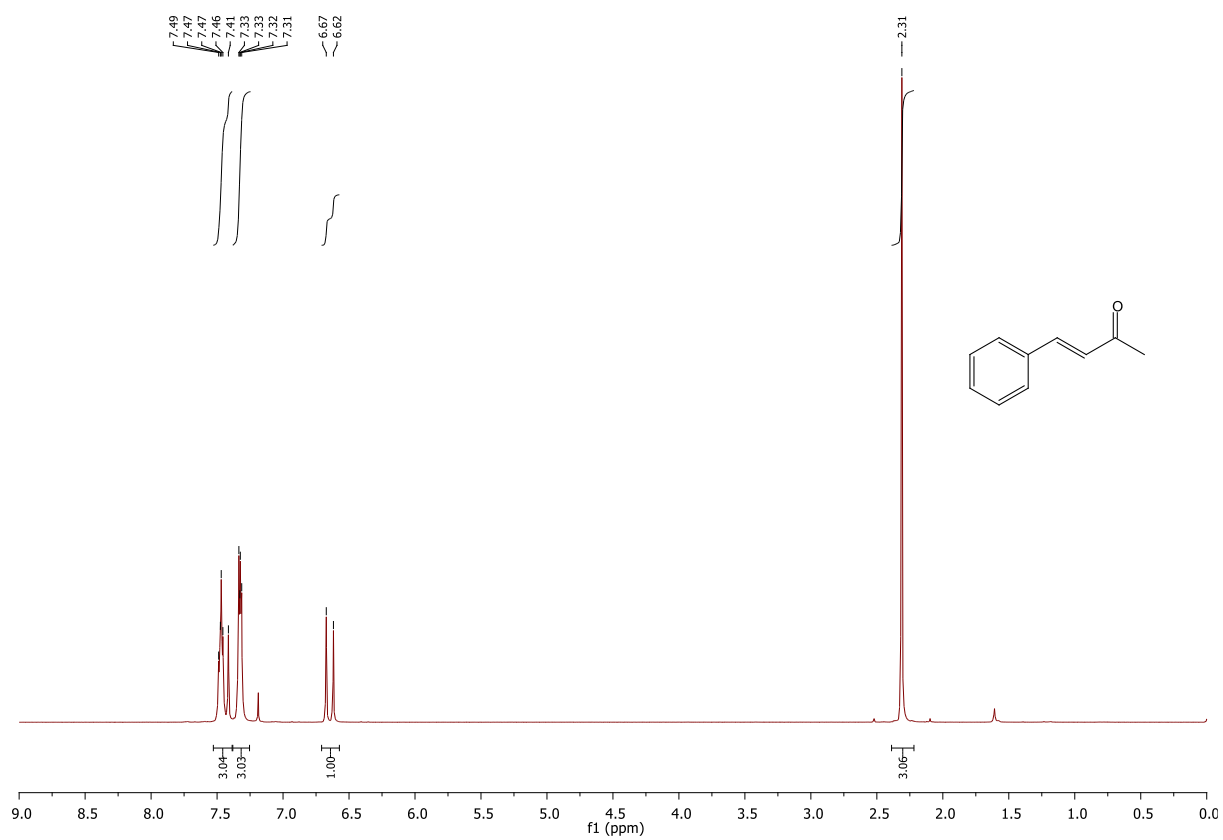
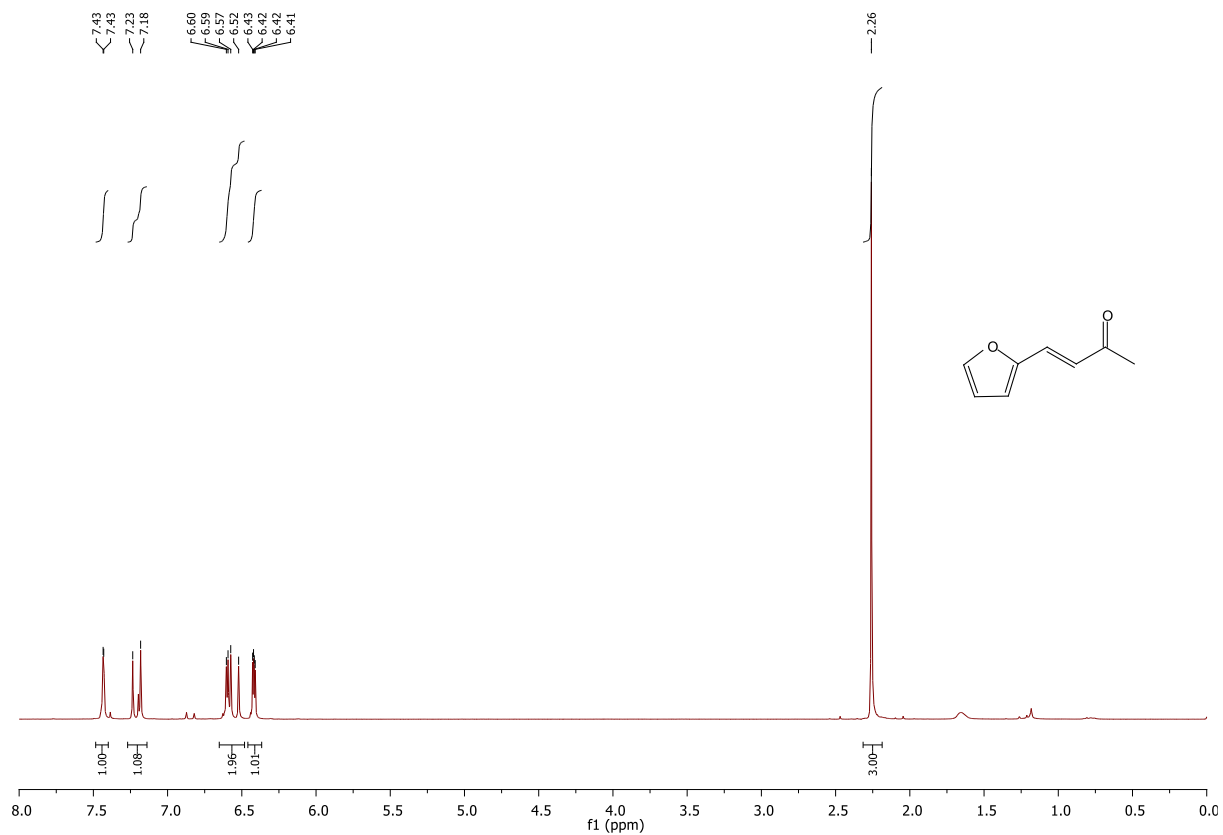


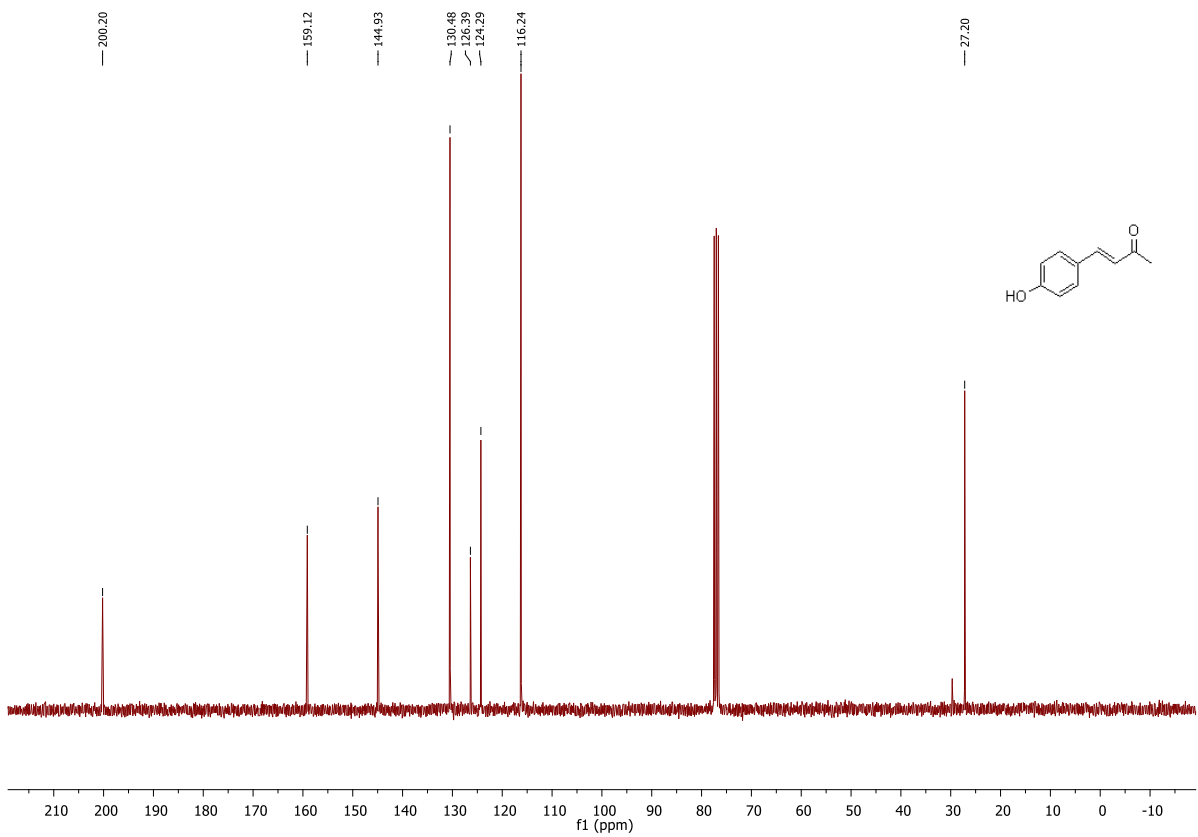
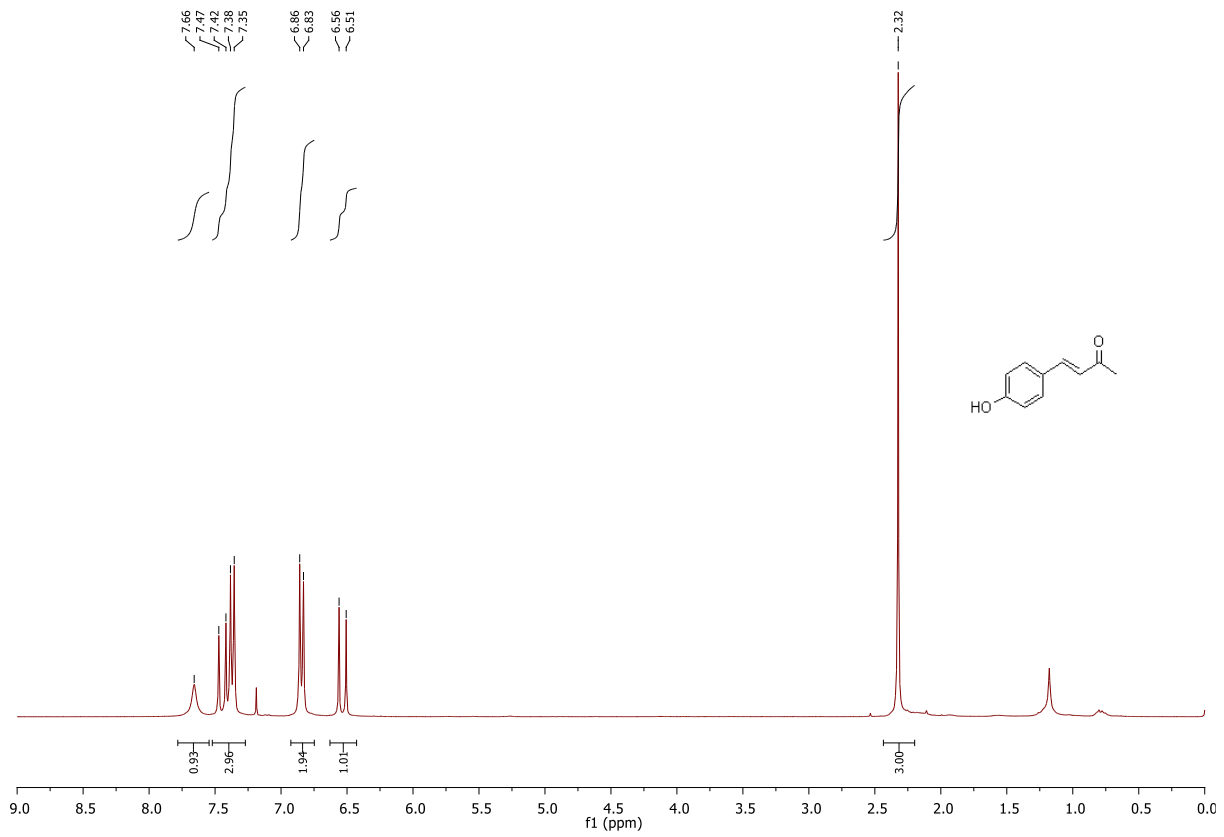
**Figure S38.** N<sub>2</sub> adsorption isotherm of Pd@Hf-MOF-808 sample after utilization in 5 consecutive runs.

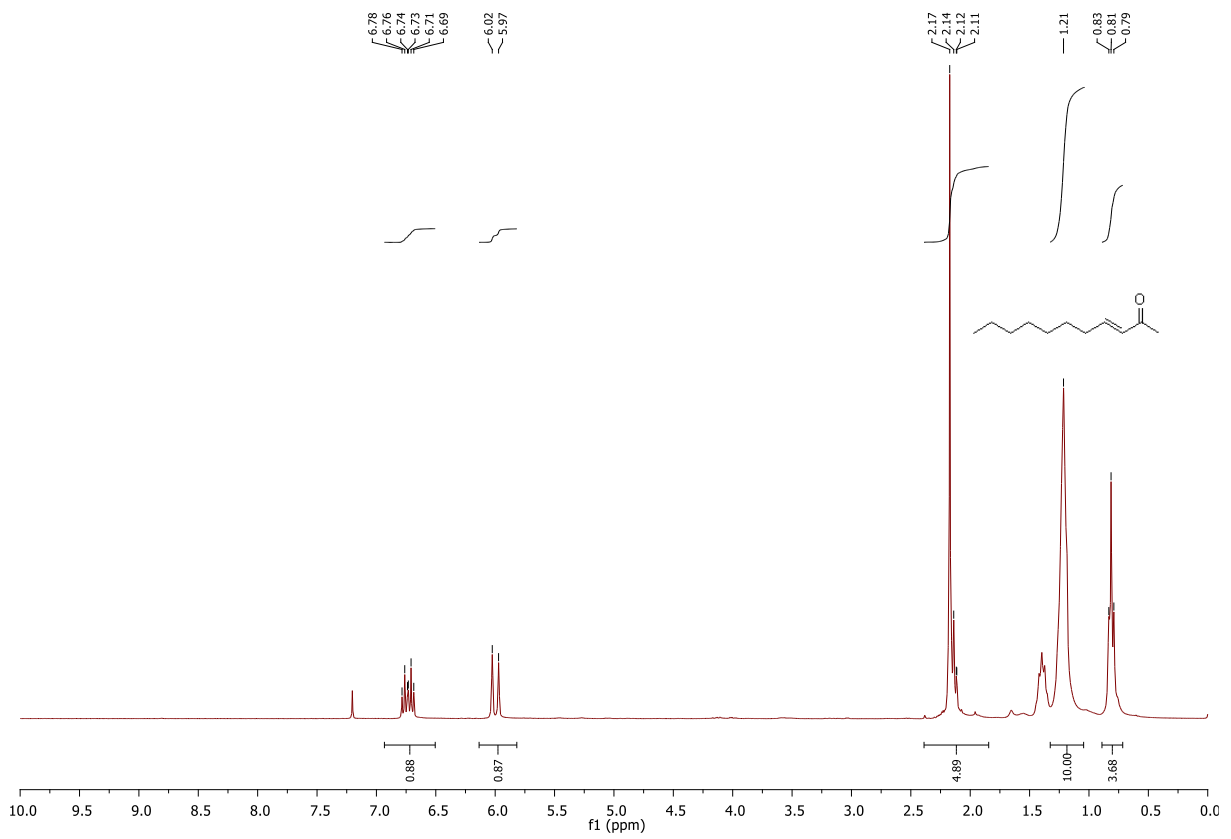
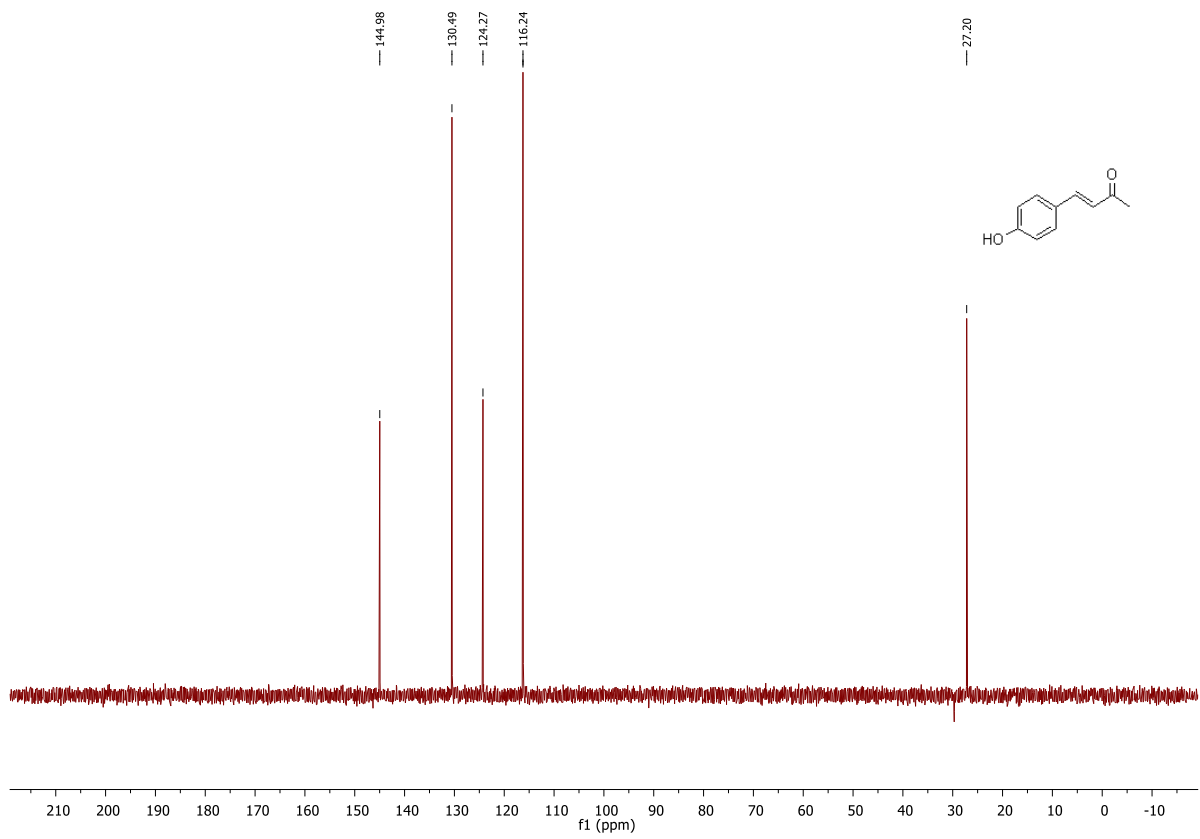
**Table S19.** Textural Characteristic of Pd@Hf-MOF-808 after utilization in 5 consecutive runs.

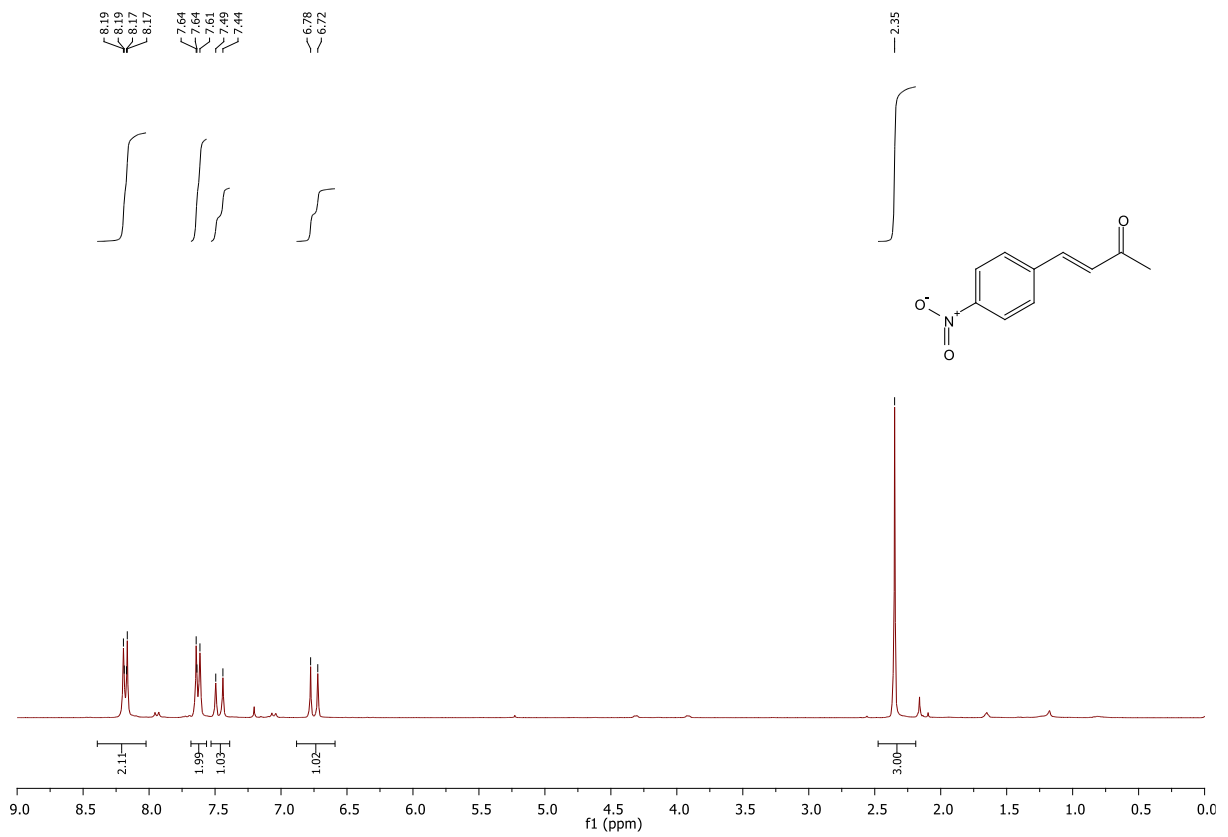
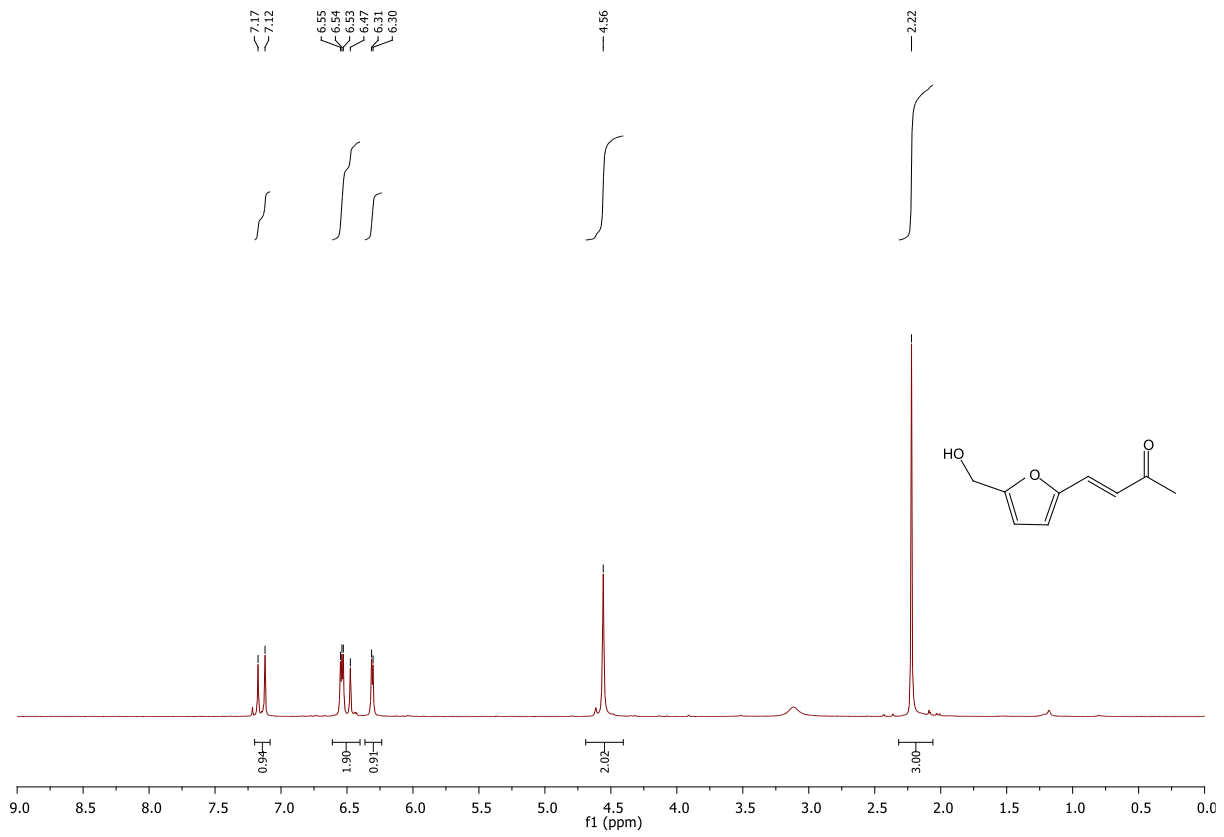
Sample	BET Surface Area/m <sup>2</sup> g <sup>-1</sup>	Total Pore Volume/cm <sup>3</sup> g <sup>-1</sup>
Pd@Hf-MOF-808 after 5 uses	74	0.12

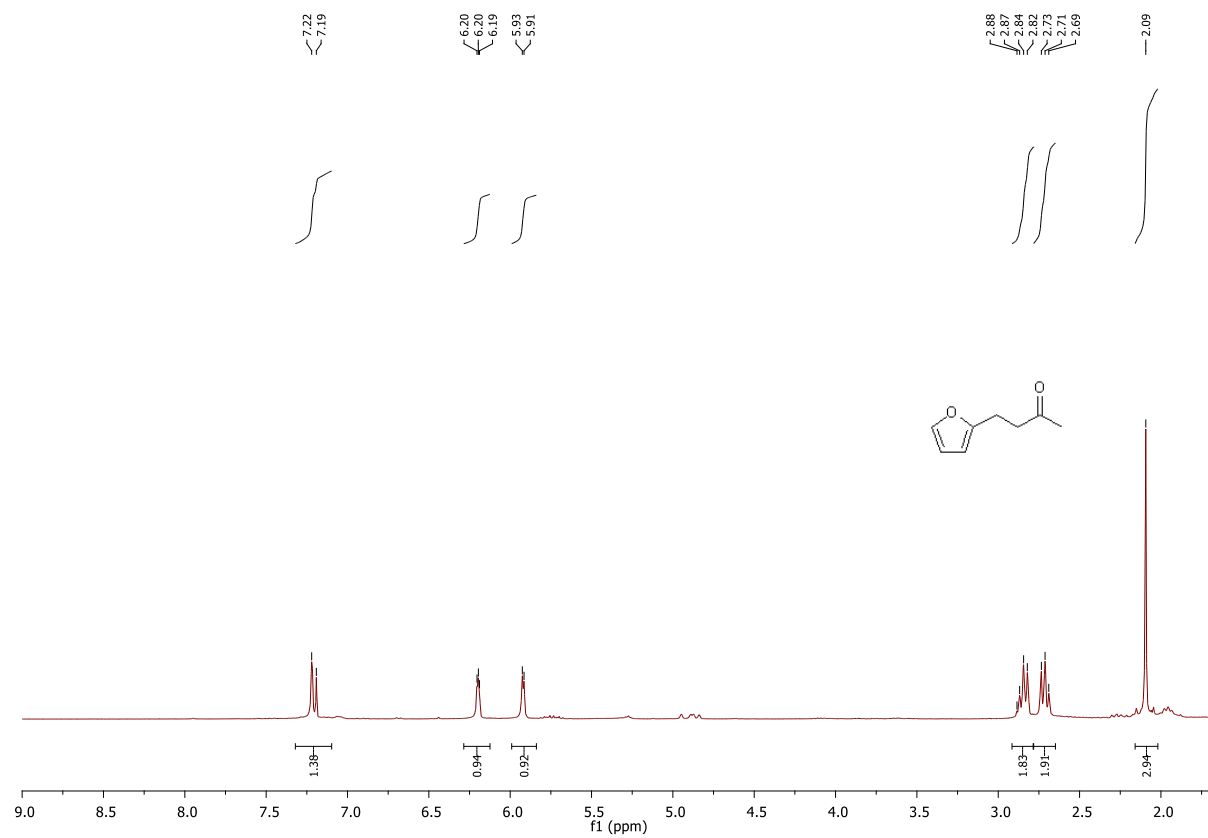
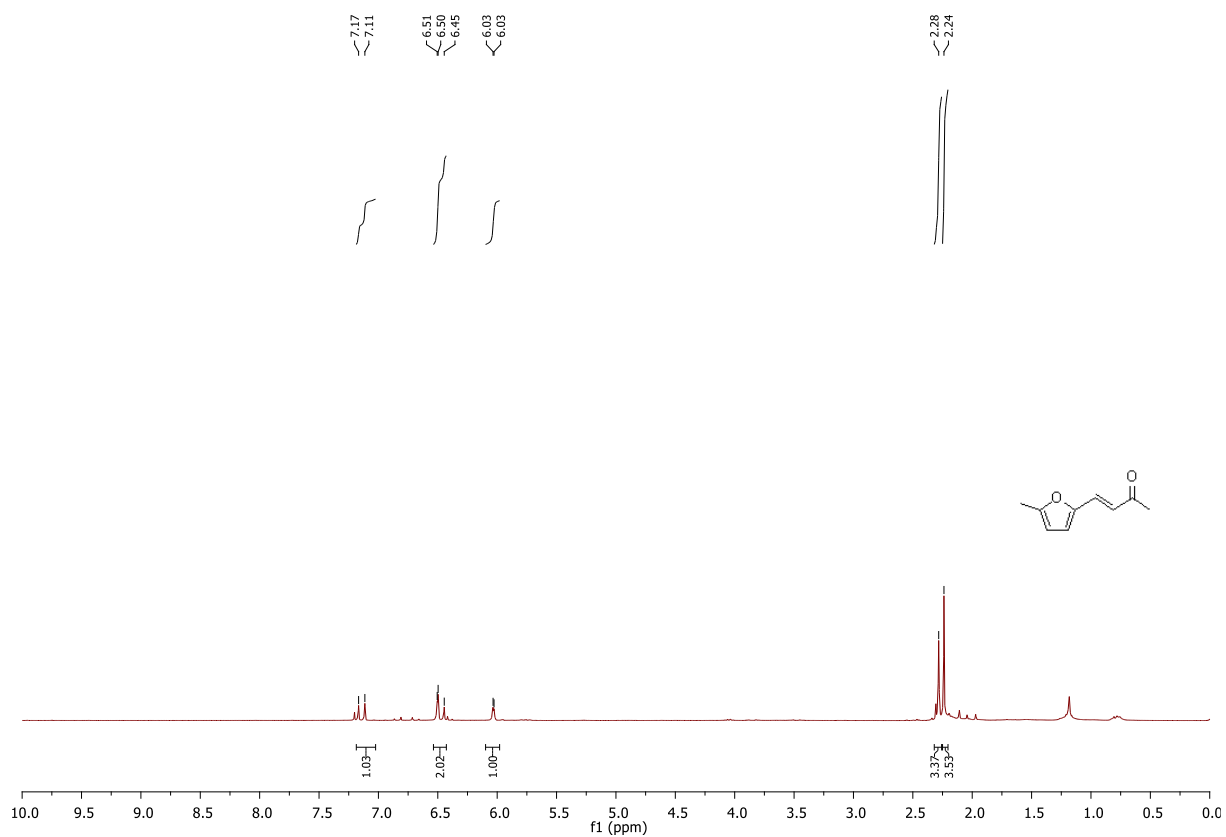
# $^1\text{H}$ and $^{13}\text{C}$ NMR spectra.

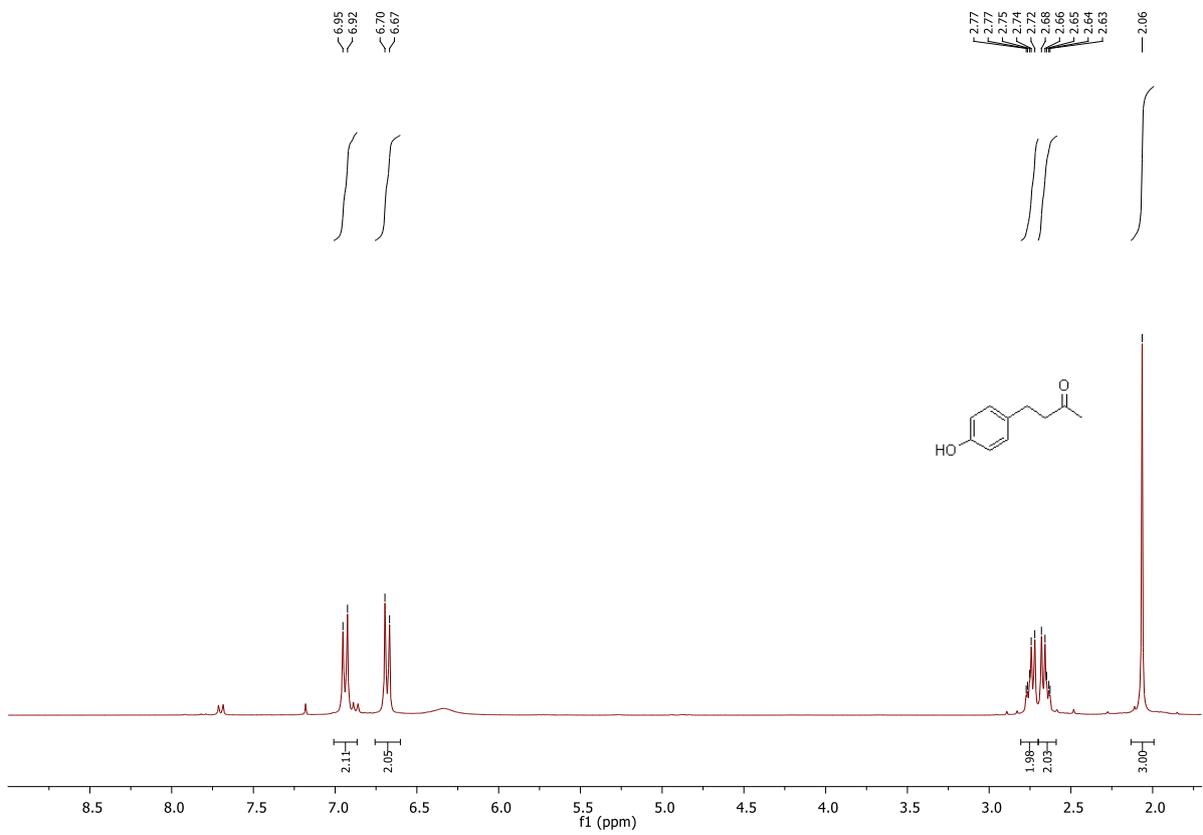
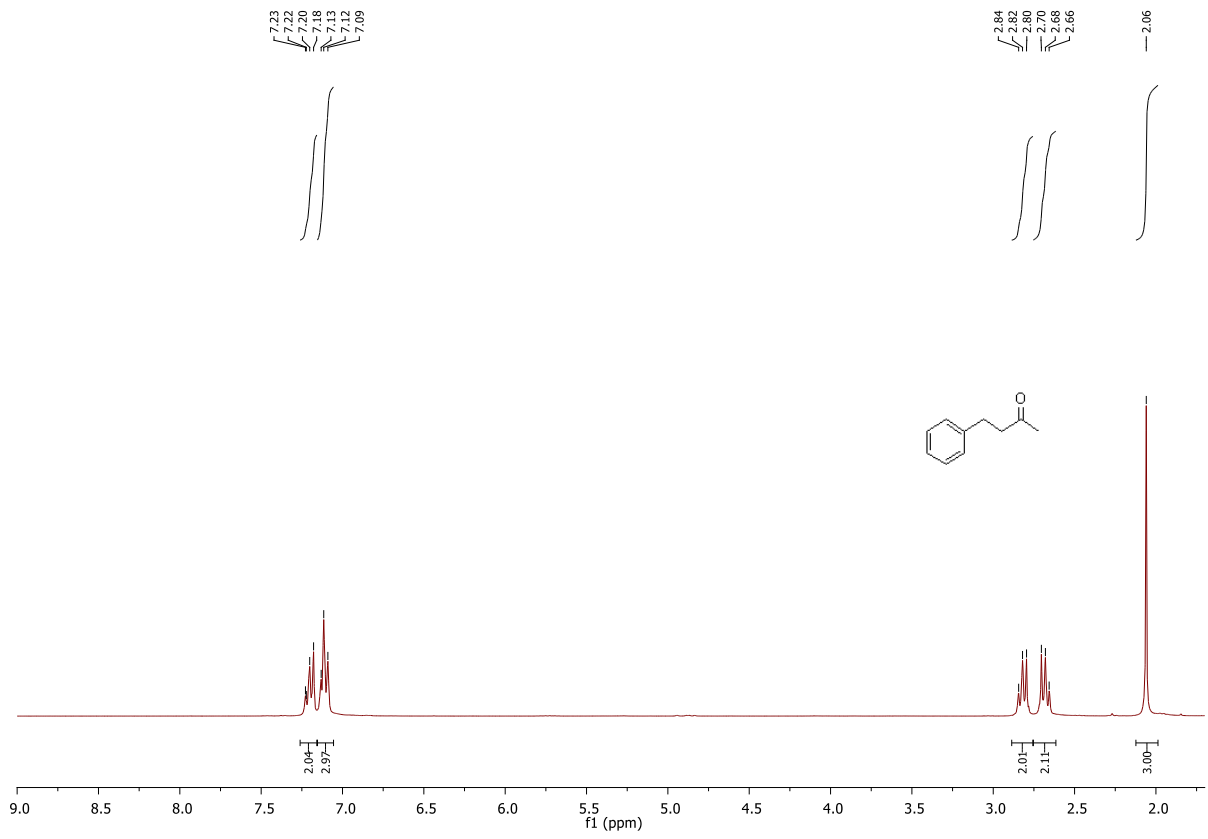












## References:

- [1] M. J. Cliffe, W. Wan, X. Zou, P. A. Chater, A. K. Kleppe, M. G. Tucker, H. Wilhelm, N. P. Funnell, F.-X. Coudert, A. L. Goodwin, *Nat. Commun.* **2014**, *5*, 4176.
- [2] Y. Liu, R. C. Klet, J. T. Hupp, O. Farha, *Chem. Commun. (Cambridge, U. K.)* **2016**, *52*, 7806-7809.
- [3] M. N. Timofeeva, V. N. Panchenko, J. W. Jun, Z. Hasan, M. M. Matrosova, S. H. Jung, *Applied Catalysis A: General* **2014**, *471*, 91-97.
- [4] S. Rojas-Buzo, P. Garcia-Garcia, A. Corma, *ChemSusChem* **2017**, Ahead of Print.
- [5] X. Li, L. Li, Y. Tang, L. Zhong, L. Cun, J. Zhu, J. Liao, J. Deng, *The Journal of Organic Chemistry* **2010**, *75*, 2981-2988.
- [6] H. Quiroz-Florentino, R. Aguilar, B. M. Santoyo, F. Díaz, J. Tamariz, *Synthesis* **2008**, *2008*, 1023-1028.
- [7] A. L. Gottumukkala, J. F. Teichert, D. Heijnen, N. Eisink, S. van Dijk, C. Ferrer, A. van den Hoogenband, A. J. Minnaard, *The Journal of Organic Chemistry* **2011**, *76*, 3498-3501.
- [8] N. Solin, L. Han, S. Che, O. Terasaki, *Catalysis Communications* **2009**, *10*, 1386-1389.
- [9] R. Gomes, A. M. Diniz, A. Jesus, A. J. Parola, F. Pina, *Dyes and Pigments* **2009**, *81*, 69-79.
- [10] M. Viviano, T. N. Glasnov, B. Reichart, G. Tekautz, C. O. Kappe, *Organic Process Research & Development* **2011**, *15*, 858-870.